ORGANOMETALLICS

Article

pubs.acs.org/Organometallics

{Phenoxy-imine}aluminum versus -indium Complexes for the Immortal ROP of Lactide: Different Stereocontrol, Different Mechanisms

Mickael Normand,[†] Vincent Dorcet,[‡] Evgeny Kirillov,[†,*] and Jean-François Carpentier[†,*]

[†]Organometallics: Materials and Catalysis and [‡]Centre de Diffractométrie X, Institut des Sciences Chimiques de Rennes, UMR 6226 CNRS-Université de Rennes 1, F-35042 Rennes Cedex, France

Supporting Information

ABSTRACT: A series of dialkylaluminum and -indium $\{ON^R\}MR'_2$ complexes (M = Al, R′ = Me; M = In, R′ = Me, CH_2SiMe_3) stabilized by a phenoxy-imine $\{ON^R\}^-$ ligand platform, with variable R-imino substituents and functionalized by a bulky *o*-$SiPh_3$ in the phenoxy moiety, has been prepared and structurally characterized in solution and in the solid state. $\{ON^R\}AlMe_2$ complexes reacted with alcohols, in particular with alkyl (*S*)-H-lactate, to generate the corresponding $\{ON^R\}Al(OR)_2$ compounds. On the other hand, the indium complexes $\{ON^R\}InR'_2$ proved largely inert toward alcohols. When they were combined with an alcohol (*i*PrOH, BnOH), the $\{ON^R\}AlMe_2$ complexes promoted the living (*immortal*) ring-opening polymerization ((*i*)ROP) of racemic lactide (*rac*-LA) with a good control over the molecular weights and various microstructures, dependent on the R-imino substituent. Complexes having benzyl-type imino substituents enabled the achievement of significant isotacticity (P_m up to 0.80), following grossly the bulkiness of the aryl moiety. The analogous $\{ON^R\}InR'_2$ proved similarly active for the (*i*)ROP of *rac*-LA in presence of an external alcohol, but the polymerizations were less controlled and none of the complexes induced stereoselectivity, except one (**3a**, P_m = 0.70). Kinetic studies revealed different rate laws, with an apparent zero-order dependence on monomer for the aluminum system **1m**/*i*PrOH and a first-order dependence on monomer for the analogous indium system **3m**/*i*PrOH. On the basis of the stoichiometric reactivity of model compounds, two different operative ROP mechanisms are suggested, depending on the nature of the metal center: Al-based complexes proceed through coordination−insertion, while In-based complexes are proposed to operate through an activated monomer mechanism.

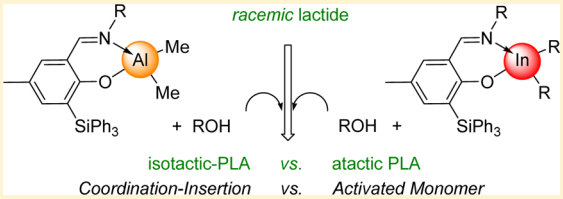

INTRODUCTION

Intensive efforts have been devoted over the past two decades to the development of metal-based catalysts able to achieve the stereoselective and controlled (*immortal*) ring-opening polymerization ((*i*)ROP) of *rac*-lactide (*rac*-LA).[1] In this regard, aluminum complexes have demonstrated attractive performance, with the possibility to access PLAs with a wide range of iso-/heterotacticities, notably with salen,[2] dialkoxy-diimino,[3] salan,[4] or salalen[5] $\{ONNO\}^{2-}$ tetradentate ligand platforms (Figure 1). On the other hand, aluminum derivatives of bidentate phenoxy-imine $\{ON\}^-$ ligands were also shown to be effective in the ROP of LA, but the examples of such hemisalen compounds developed thus far did not offer noticeable stereocontrol when applied to *rac*-LA (P_m up to 60%).[6,7]

Within the same group of elements, indium(III)-based initiators[8−12] have been more recently explored for the ROP of *rac*-LA and other cyclic esters (*ε*-caprolactone, *β*-butyrolactone).[13] The catalytic performances of these compounds were contrasted, however; in fact, quite a few systems[8] revealed valuable activity and high stereoselectivity. In a recent study, we prepared a series of fluorinated dialkoxy-diimino $\{ON^RNO^{CF3}\}InX$ compounds (X = O*i*Pr, alkyl) and showed that they are significantly less stereoselective than their $\{ON^RNO^{CF3}\}AlX$ analogues in the ROP of *rac*-LA.[14] This was tentatively proposed to arise, at least in part, from the larger size of the indium center,[15] which might generate less sterically crowded coordination environments around the active metal center. It is indeed well-accepted that organometallic compounds usually play a crucial assistance in chain-end-controlled ROP processes, with evidence that subtle ligand/metal modifications may result in very important effects on stereoselectivity.[16] However, possible fundamental differences in the operative ROP mechanism (i.e., coordination−insertion vs activated monomer pathways) when shifting from aluminum to the relatively more covalent and less Lewis acidic indium compounds were also questioned.

Herein we report a series of dialkyl and dialkoxy {phenoxy-imine}aluminum and -indium complexes and their use as catalysts/initiators for the (*i*)ROP of *rac*-LA. Our aim was to compare the performance of these $\{ON\}InX_2$ complexes in terms of activity, as well as molecular weight and stereochemical control, with that of their aluminum congeners. For this purpose, we used a phenoxy-imine $\{ON\}^-$ ligand platform, with variable R-imino substituents, functionalized in the phenoxy moiety by a *o*-triphenylsilyl moiety,[17] in order to

Received: November 28, 2012

   dx.doi.org/10.1021/om301155m | *Organometallics* XXXX, XXX, XXX−XXX

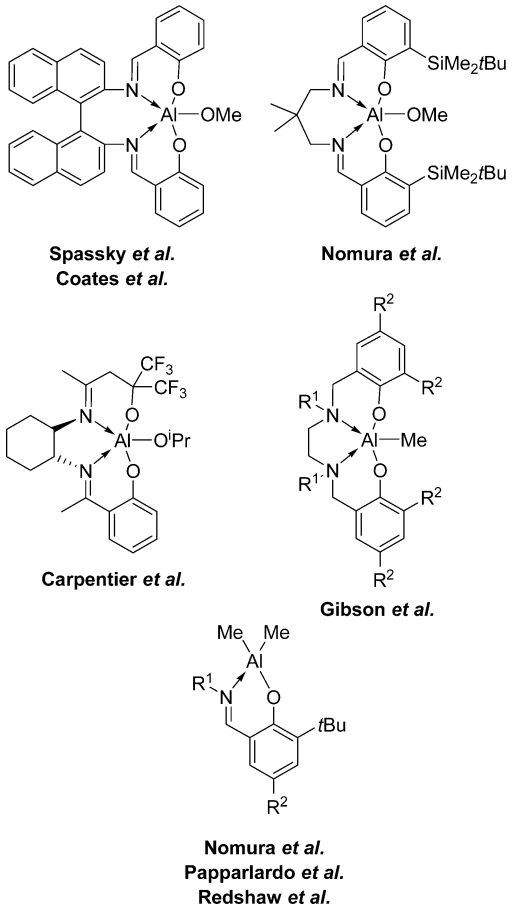

Figure 1. Examples of aluminum (pre)catalysts based on tetradentate $\{ONNO\}^-$ and bidentate $\{ON\}^-$ ligands for the ROP of racemic lactide.

enhance the hindrance around the metal center and to prevent any aggregation phenomena (Figure 2). It is shown that

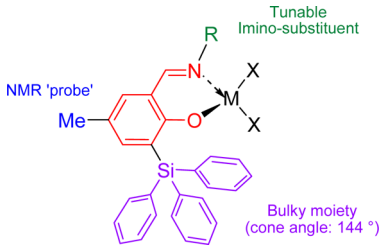

Figure 2. Structure of the {phenoxy-imino}metal platform used in this study.

modulation of the R-imino substituents in the $\{ON\}AlMe_2$ complexes allowed control of the stereoselectivity of the ROP, from highly isoselective to heteroselective systems, with improved performance in comparison to the related {phenoxy-imine}aluminum systems thus far reported. A change in the operative mechanism between aluminum- and indium-based catalysts is also highlighted.

RESULTS AND DISCUSSION

Synthesis of Proligands. Three main categories of phenol-imine proligands (**a**–**m**, Table 1)) were explored: (1) potentially tridentate ($\{ONN^{qui}\}H$ (**a**) and $\{ONN^{CH2pyr}\}H$ (**g**)) proligands, (2) bidentate proligands that tune the bulkiness of the phenyl ring (**b**–**e**) directly bonded to the nitrogen of the imino moiety, and (3) bidentate proligands that possess a *N*-benzyl-type group substituted at either the CH_2 linker or the phenyl ring (**f**, **h**–**k**). These proligands **a**–**m** were prepared from 2-hydroxy-5-methyl-3-(triphenylsilyl)-benzaldehyde[18] and the corresponding primary amine, using two different protocols[19] (Scheme 1). Compounds **a**–**m** were obtained in 26–62% isolated yields after recrystallization as analytically pure yellow (red for **a**) crystalline powders (Table 1). They were authenticated by elemental analysis, ^1H, $^{13}C\{^1H\}$, and $^{19}F\{^1H\}$ (when relevant) NMR spectroscopy (see the Experimental Section), and X-ray diffraction studies for **f**, **e**, and **l** (see the Supporting Information)

Synthesis of {Phenoxy-imine}aluminum and -indium Complexes. Dimethylaluminum complexes were prepared in good yields (50–83%) by treatment of the appropriate Schiff base proligand with a stoichiometric amount of $AlMe_3$. The reaction took place in dry toluene at room temperature with concomitant elimination of 1 equiv of methane (Scheme 1). The synthesis of dialkylindium complexes was achieved also by protonolysis using two different precursors, namely $[InMe_3]_n$ generated in situ from $InCl_3$ and MeLi[20] and the discrete homoleptic precursor $In(CH_2SiMe_3)_3$ (Scheme 1).[21] The former protonolysis reaction proved selective only toward two proligands, namely $\{ONN^{qui}\}H$ (**a**) and $\{ON^{pipeBn}\}H$ (**m**), resulting in the corresponding dimethylindium complexes $\{ONN^{qui}\}InMe_2$ (**2a**) and $\{ON^{pipeBn}\}InMe_2$ (**2m**), isolated in 47% and 77% yields, respectively. When the same reaction was conducted with the other proligands, complex mixtures of starting materials and unidentified products were observed. In contrast, the reactions of the tricarbyl precursor $In(CH_2SiMe_3)_3$ with the six proligands tested (**a**, **f**–**h**, **l**, and **m**) yielded selectively the corresponding dicarbylindium derivatives **3a**,**f**–**h**,**l**,**m** as bright yellow crystalline solids.

The structures of these complexes were established on the basis of ^1H and $^{13}C\{^1H\}$ NMR spectroscopy and elemental analysis and by single-crystal X-ray diffraction studies for **1f**,**g**,**m**, **2a**,**m**, and **3a**.[22]

The ^1H NMR spectra of complexes **1a**–**m**, **2a**,**m**, and **3a**–**m** in C_6D_6 at room temperature contain all single sets of sharp resonances that are consistent with monomeric structures in solution (as observed in the solid state; vide infra). Expectedly, in the aluminum and indium complexes bearing a chiral substituent, $\{ON^{CMetBu}\}AlMe_2$ (**1l**) and $\{ON^{CMetBu}\}In(CH_2SiMe_3)_2$ (**3l**), two sets of close but distinct singlets were observed for the inequivalent methyl and CH_2SiMe_3 groups (see the Experimental Section).

The solid-state molecular structures of aluminum complexes $\{ON^{pipeBn}\}AlMe_2$ (**1m**) and $\{ONN^{CH2pyr}\}AlMe_2$ (**1g**) are shown in Figures 3 and 4, respectively (see Figure S2 in the Supporting Information for that of **1f**). Values of relevant bond distances and angles are given in Table 2. Complexes **1f**,**m**, which bear bidentate ligands, feature a four-coordinated aluminum center in a distorted-tetrahedral geometry (bond angles (C(1_1)–Al–C(1_2) = 122.96(6) and 123.10(4)°, O(1)–Al–C(1_1) = 109.74(8) and 109.47(11)°, and O(1)–Al–C(1_2) = 109.03(8) and 109.45(12)°, respectively). On the other hand, the aluminum center in the five-coordinated complex **1g**, which has a tridentate ligand, lies in a highly distorted trigonal bipyramidal geometry (τ = 0.65).[23] Of note, the piperidinyl ring moiety in complex **1m** remains in a boat conformation with no coordination of the nitrogen to the metallic center. The Al–C (1.951(2)–1.973(3) Å), Al–O

dx.doi.org/10.1021/om301155m | *Organometallics* XXXX, XXX, XXX–XXX

Table 1. Synthetic Route toward Phenol-(R substituted)imine Proligands $\{ON^{R}\}H$

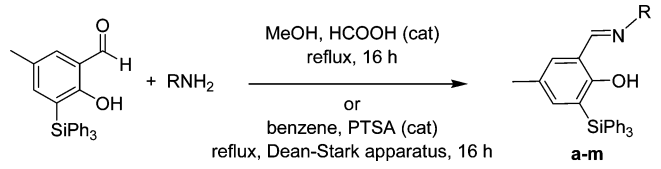

a-m

label	abbreviation	Imine substituent R		Protocol[a]	Yield (%)
a	$\{ONN^{qui}\}H$	8-quinolyl		A	62
b	$\{ON^{PhiPr2}\}H$	2,6-di-*i*Pr-phenyl	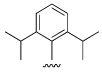	B	41
c	$\{ON^{ArF}\}H$	3,5-di-CF_3-phenyl		A	58
d	$\{ON^{ArCF3}\}H$	2,6-(3,5-bis(trifluoromethyl)phenyl)phenyl	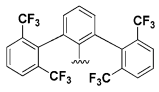	A	26
e	$\{ON^{Phmorpho}\}H$	2-morpholinephenyl	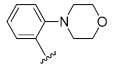	A	60
f	$\{ON^{Bn}\}H$	benzyl		A	43
g	$\{ONN^{CH2pyr}\}H$	CH_2(2-pyridyl)		B	31
h	$\{ON^{CH2mes}\}H$	CH_2-mesityl	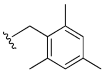	A	61
i	$\{ON^{BnOMe3}\}H$	CH_2-3,4,5-trimethoxyphenyl		A	37
j	$\{ON^{CHPh2}\}H$	benzal		A	27
k	$\{ON^{trityl}\}H$	trityl		A	38
l	$\{ON^{CMetBu}\}H$	(*R*)-3,3-dimethyl-2-butyl		A	52
m	$\{ON^{pipeBn}\}H$	*N*-benzyl-4-piperidinyl	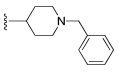	A	62

[a]Protocol A: MeOH, HCOOH (cat.), reflux, 16 h. Protocol B: benzene, PTSA (cat.), reflux, Dean−Stark.

(1.772(2)−1.861(2) Å), and C═N (1.9703(16)−2.027(3) Å) distances in compounds **1f,g,m** are in the range of bond lengths observed in the {phenoxy-imine}aluminum complex $Me_2Al[O\text{-}2\text{-}tBu\text{-}6\text{-}\{(2,4,6\text{-}Me_3C_6H_2)N{=}CH\}C_6H_3]$ reported by Nomura et al.[4a] (1.953(2)−1.956(2), 1.7748(19), and 1.965(2) Å, respectively).

Complex $\{ON^{pipeBn}\}InMe_2$ (**2m**) crystallizes with the indium center in a distorted-tetrahedral coordination and is isostructural with its aluminum congener (see Figure 5 and Figure S3 (Supporting Information)). The five-coordinated indium complexes $\{ONN^{qui}\}InMe_2$ (**2a**) and $\{ONN^{qui}\}In(CH_2SiMe_3)_2$ (**3a**) are isostructural, and their highly distorted coordination environments fall just between trigonal bipyramidal and square pyramidal (τ = 0.51 for both compounds, Figure S4 (Supporting Information) and Figure 5, respectively). The In−O, In−C, and In−N bond distances of these three complexes (Table 2) are to some extent larger than those observed in the five-coordinated {diaminophenoxy}-dimethylindium derivative $\{NN_HO\}InMe_2$ described by Mehrkhodavandi and co-workers (2.152(2), 2.161(2)−2.150(2), and 2.355(2)−2.503(2) Å, respectively).[24]

dx.doi.org/10.1021/om301155m | *Organometallics* XXXX, XXX, XXX−XXX

Scheme 1. Synthetic Routes toward {phenoxy-imine}$AlMe_2$ Complexes (Route 1), {phenoxy-imine}$InMe_2$ Complexes (Route 2), and {phenoxy-imine}$In(CH_2SiMe_3)_2$ Complexes (Route 3)

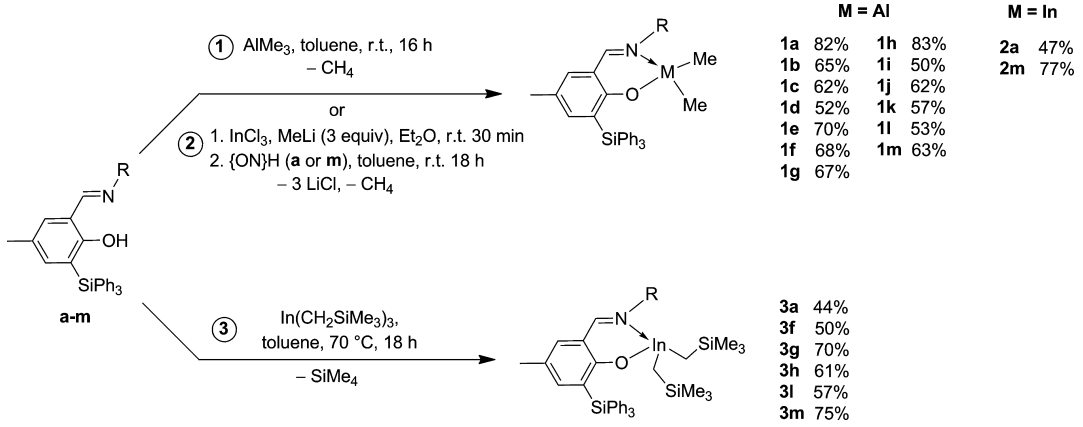

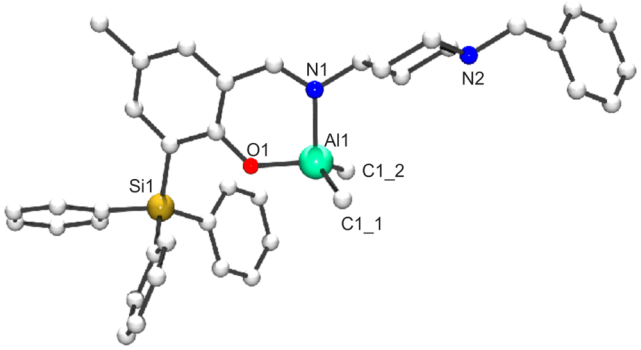

Figure 3. Solid-state molecular structure of {ON^{pipeBn}}$AlMe_2$ (**1m**). All hydrogen atoms are omitted for clarity.

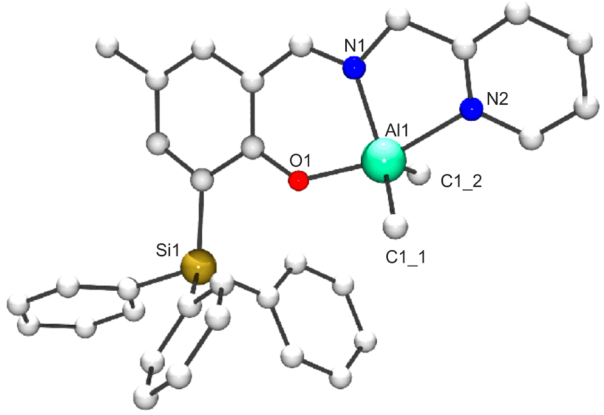

Figure 4. Solid-state molecular structure of {ONN^{CH2pyr}}$AlMe_2$ (**1g**). All hydrogen atoms are omitted for clarity.

Reactivity of {Phenoxy-imine}aluminum and -indium Dialkyl Complexes toward Alcohols. Typical metal-based catalysts/initiators for the ROP of lactones incorporate one (or more) alkoxide group which is capable of rapid and efficient initiation.[1] This alkoxide either is initially present as a discrete alkoxy complex or, more commonly, is formed in situ by the reaction between an exogenous alcohol and an alkyl(amido) metal precursor. The latter is actually the route that was followed earlier by the groups of Nomura and Pellechia, and more recently by Redshaw, with {phenoxy-imine}$AlMe_2$ compounds, although the exact nature of the active ROP species was not addressed.[6a−c] Recently, we have reported in detail on the reactivity of the complexes {ONN^{qui}}$AlMe_2$ (**1a**), {ON^{Bn}}$AlMe_2$ (**1b**), and {ONN^{CH2pyr}}$AlMe_2$ (**1c**) toward *i*PrOH.[25] We have shown that the last two compounds lead to the monoalkoxides {ON^{Bn}}$_2$Al(O*i*Pr) (**5b**) and {ONN^{CH2pyr}}$_2$Al(O*i*Pr) (**5c**), respectively, as the major products, along with other unidentified species (Scheme 2). Unexpectedly, for **1a**, which contains an {ONN^{qui}}$^-$ ligand system with an electron-withdrawing N substituent, occurrence of deleterious (although totally selective) Meerwein−Ponndorf−Verley (MPV) reduction at the imino functionality was evidenced; [{ONN^{qui}}{$ON^{H}N^{qui}$}Al] (**6a**), which contains a monoanionic {ONN^{qui}}$^-$ ligand and another dianionic ligand ({$ON^{H}N^{qui}$}$^{2-}$) that results from the reduction of the latter imino group into an amido moiety, was thus recovered.[25] On the other hand, our attempts to convert dialkylaluminum complexes **1d**,**e**,**h**−**m** into alkoxy complexes, via treatment with 2−5 equiv of *i*PrOH in a polar solvent (THF) or in aromatic hydrocarbons (benzene, toluene) over a wide range of temperatures (−20 to +80 °C), resulted in intractable mixtures of products and no clear evidence of actual generation of alkoxide species was gained (Scheme 2); even release of the proligands was observed in some cases.

Alternative routes toward well-defined aluminum alkoxy type species using H-lactates instead of isopropyl alcohol were investigated. Bis(*α*-alkoxy ester)aluminum derivatives were synthesized cleanly by reacting {ONN^{qui}}$AlMe_2$ (**1a**) with 2 equiv of (1*R*,2*S*,5*R*)-menthyl (*S*)-lactate and by reacting {ON^{Bn}}$AlMe_2$ (**1f**) as well as {ON^{pipeBn}}$AlMe_2$ (**1m**) with 2 equiv of isopropyl (*S*)-lactate, to give {ONN^{qui}}Al(menthyl (*S*)-lactate)$_2$ (**7a**), {ON^{Bn}}Al(*i*Pr (*S*)-lactate)$_2$ (**8f**), and {ON^{pipeBn}}Al(*i*Pr (*S*)-lactate)$_2$ (**8m**), which were isolated in 30%, 70%, and 82% yields, respectively (Scheme 3). These complexes were characterized on the basis of 1D and 2D ^{1}H and ^{13}C{^{1}H} NMR spectroscopy and elemental analysis. Repeated attempts to grow X-ray-quality crystals were unfortunately unsuccessful. Still, these constitute to our knowledge the first examples reported of {phenoxy-imine}aluminum lactate complexes.[26]

The ^{1}H NMR spectra of {ON^{Bn}}Al(*i*Pr (*S*)-lactate)$_2$ (**8f**) and {ON^{pipeBn}}Al(*i*Pr (*S*)-lactate)$_2$ (**8m**) in benzene-d_6 at room temperature are similar (Figures A53 and A56 in the Supporting Information). The observation of a series of sharp resonances in both cases is consistent with the existence of single monomeric species in solution. In particular, the methyl phenoxy hydrogens—used as an NMR probe—come out as

dx.doi.org/10.1021/om301155m | *Organometallics* XXXX, XXX, XXX−XXX

Table 2. Selected Bond Distances (Å) and Angles (deg) for Complexes 1f,g,m, 2a,m, and 3a

	$\{ON^{Bn}\}AlMe_2$ (1f)	$\{ON^{pipeBn}\}AlMe_2$ (1m)	$\{ON^{CH2pyr}\}AlMe_2$ (1g)	$\{ONN^{qui}\}InMe_2$ (2a)	$\{ONN^{qui}\}InCH_2SiMe_3$ (3a)	$\{ON^{pipeBn}\}InMe_2$ (2m)
M−C(1_1)	1.951(2)	1.963(3)	1.979(3)	2.161(2)	2.162(2)	2.139(2)
M−C(1_2)	1.952(2)	1.958(3)	1.973(3)	2.147(2)	2.170(2)	2.140(2)
M−O(1)	1.778(1)	1.772(2)	1.861(2)	2.193(1)	2.198(1)	2.101(1)
M−N(1)	1.970(2)	1.992(2)	2.027(3)	2.339(2)	2.266(2)	2.268(2)
M−N(2)			2.184(3)	2.383(2)	2.471(2)	
C=N(1)	1.290(2)	1.299(3)	1.304(3)	1.309(3)	1.325(3)	1.288(2)
O(1)−M−N(1)	93.67(6)	94.71(9)	87.3(1)	80.32(6)	79.93(5)	85.33(5)
O(1)−M−N(2)			161.9(1)	150.77(6)	149.08(6)	
O(1)−M−C(1_1)	109.74(8)	109.5(1)	95.8(1)	101.27(8)	99.87(7)	103.10(8)
O(1)−M−C(2_2)	109.03(8)	109.5(1)	99.1(1)	96.68(8)	98.24(7)	101.19(8)

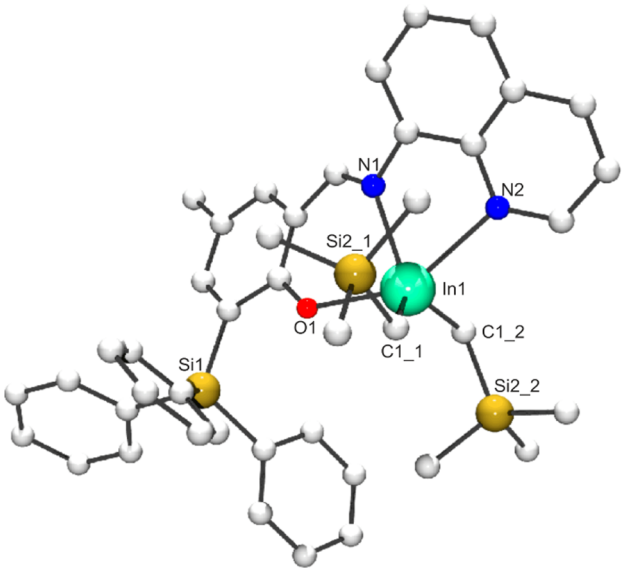

Figure 5. Solid-state molecular structure of $\{ONN^{qui}\}In(CH_2SiMe_3)_2$ (3a). All hydrogen atoms are omitted for clarity.

Scheme 2. Fate of $\{ON^R\}AlMe_2$ Compounds 1a−m on Treatment with Isopropyl Alcohol

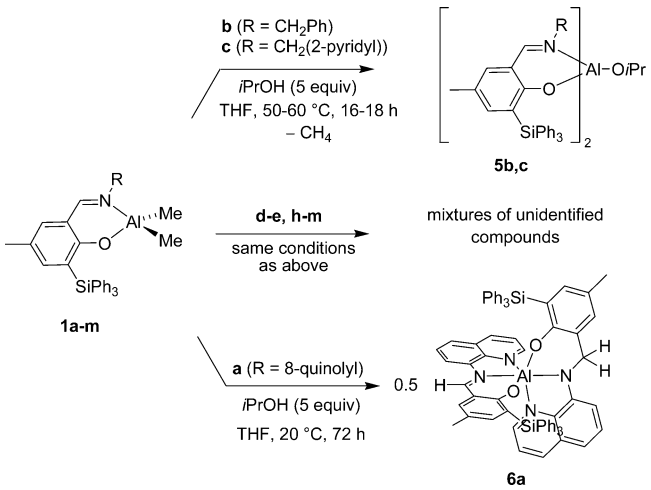

singlets (δ 1.80 and 1.95 ppm, respectively). In compounds **8f,m**, the two lactate moieties are magnetically inequivalent, as indicated by a series of six doublets (some of them partially overlap), assigned to the methyl groups and two heptets and two quartets for the methine hydrogens of the *i*Pr and lactate moieties, respectively.

The reactivity of indium complexes was also investigated (Scheme 4). Dimethyl (**2a,m**) and bis((trimethylsilyl)methyl) (**3a,f−h,l,m**) complexes were thus mixed with 2 equiv of *i*PrOH in toluene or THF at reflux; similar reactions with *i*Pr (*S*)-H-lactate were also attempted. Indium complexes **3f−h,l,m**, whatever the conditions used, appeared to be reluctant to any protonolysis reaction and remained intact after several hours. In the case of **2m**, partial release of the proligand was the main reaction observed. On the other hand, both complexes bearing the 8-quinolyl imino substituent (**2a** and **3a**) specifically reacted as their aluminum analogue **1a**, via MPV reduction of the imino functionality, to generate $[\{ONN^{qui}\}\{ON^{H}N^{qui}\}In]$ (**9a**).[25]

ROP of *rac*-Lactide Catalyzed by {Phenoxy-imine}-aluminum and -indium Initiators: Activity, Living Immortal Character, and Stereoselectivity. The data from a series of polymerizations of *rac*-lactide (*rac*-LA) by aluminum complexes **1a−m** in toluene solution at 100 °C are collected in Table 3.

Aluminum-Based Initiators. When they were associated with an exogenous alcohol (isopropyl alcohol or benzyl alcohol), all dimethyl{phenoxy-imine}aluminum complexes proved to be active in the ROP of *rac*-LA at 100 °C for a period of time ranging from 2 to 20 h at a [lactide]/[catalyst/initiator]/[alcohol] ratio of 100/1/1. The observed molecular weights of all the polymers produced with the aluminum complexes employed in this study, i.e., complexes **1a−m**, were found to be close to the theoretical values in the range of M_n(SEC) = 3300−11900 g mol^{-1}. All the PLAs formed under those conditions had unimodal and narrow molecular distributions (M_w/M_n = 1.10−1.24; Table 3, entries 1−22), except for complexes **1i,j,l**, for which polydispersity indices were somewhat broader (M_w/M_n = 1.51, 1.32, and 1.46, respectively; Table 3, entries 16, 17, and 19). For a given experiment, monitoring the ROP of *rac*-LA using **1f** by ^{1}H NMR spectroscopy showed that the molecular weight increased with conversion in a linear relationship in [*rac*-LA]/[Al]/[*i*PrOH] ratios of 100/1/1 and 500/1/1 (Figure 6).

The best activity obtained under optimized reaction times was reached with complex **1f**, which featured an apparent turnover frequency (TOF) of 14 mol of LA (mol of Al)$^{-1}$ h^{-1} at 100 °C. This value is similar to those achieved with {phenoxy-imine}aluminum catalyst precursors used with MeOH as a chain transfer agent (CTA) reported by Pappalardo et al.[6b] (TOF = 1.5 mol of LA (mol of Al)$^{-1}$ h^{-1} at 70 °C) and those of Nomura et al.[6a] or Redshaw et al.[6c] using *n*BuOH as a

dx.doi.org/10.1021/om301155m | Organometallics XXXX, XXX, XXX−XXX

Scheme 3. Routes toward {ON^R}bis(alkyl (*S*)-lactate)aluminum Complexes 7a and 8f,m

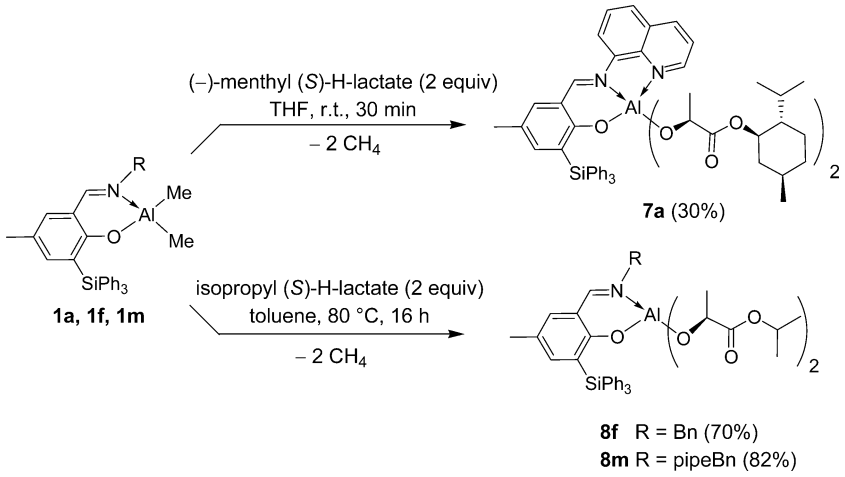

Scheme 4. Fate of {ON^R}InR′$_2$ Compounds on Treatment with Isopropyl Alcohol

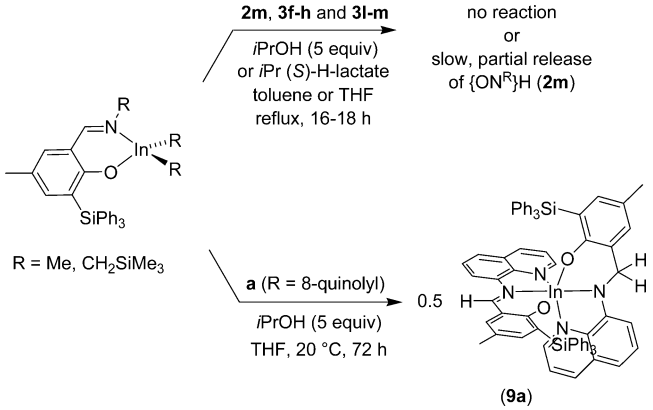

transfer agent (TOF = 4–5 mol of LA (mol of Al)$^{-1}$ h^{-1} at 80 and 100 °C, respectively).[27]

The kinetics of the ROP of *rac*-LA promoted by binary systems made up of dimethylaluminum complex **1m** in combination with *i*PrOH were studied in more detail. All reactions featured linear plots of conversion vs time to ≥80% conversion (Figures 7 and 8) (in contrast to semilogarithmic plots, which were not linear), indicating an apparent zero order in lactide. Further experiments were conducted with variable amounts of catalyst precursor and alcohol, to determine the corresponding orders in these two components. The apparent rate constants thus determined are reported in Table 4. The experimental gradient of the least-squares fitted line between ln k_{app} vs ln [Al] was 0.97(5) (R^2 = 0.999) (Figure S78, Supporting Information), indicating a first-order dependence on catalyst concentration. The same treatment for the isopropyl alcohol concentration led to a gradient of 0.23(6) (R^2 = 0.997) (Figure S79, Supporting Information). Hillmyer and Tolman have reported similarly close, but not strictly equal, to zero values for elementary orders in their ternary $InCl_3$/BnOH/NEt_3 catalyst system and eventually concluded on a formal zero-order dependence on alcohol and amine.[8] Thus, for the **1m**/*i*PrOH system, we propose the idealized rate expression $-d[rac\text{-LA}]/dt = k_{app}[LA]^0[Al]^1[i\text{PrOH}]^0$.

An apparent zero-order dependence on monomer concentration is unusual but not unprecedented: at least two examples have been recently disclosed for the ROP of ε-caprolactone promoted by aluminum[28] and zinc[29] complexes. Hillmyer and Tolman[28] have rationalized this according to a Michaelis–Menten model in which reversible binding of the cyclic ester to the metal occurs and, if $K_M \ll$ [cyclic ester] (where K_M is the Michaelis constant related to this rapid pre-equilibrium), it can lead in fact to saturation kinetics in terms of monomer concentration. Mountford and co-workers found also this model applicable to their zinc system,[29] and we assume this is also the case in the present study.

Of interesting note, the binary catalyst made up of dimethylaluminum complex **1m** in combination with *i*PrOH and the single-component system bis(*i*Pr (*S*)-lactate)aluminum complex **8m** featured roughly the same apparent rate constants at 110 °C: i.e., k_{app} = (1.1 ± 0.1) × 10^{-3} s^{-1} for **1m**/*i*PrOH ([*rac*-LA]$_0$/[Al]/[*i*PrOH]$_0$ = 500/1/5) vs (1.4 ± 0.1) × 10^{-3} s^{-1} for **8m** ([*rac*-LA]$_0$/[Al] = 200/1) (Table 4; see Figure S80 in the Supporting Information). This observation is consistent with relatively rapid and complete generation of alkoxy initiating species when dimethyl{phenoxy-imine}aluminum complexes are reacted with isopropyl alcohol and an operative coordination–insertion polymerization process in both binary and single-component systems.

Experiments conducted under the so-called "*immortal*" polymerization conditions,[1h,i] in which the alcohol is added in excess relative to the number of potential initiating groups of the complexes (i.e., 2) and acts as a CTA ([*rac*-LA]$_0$/[Al]/[*i*PrOH]$_0$ = 1000/1/10; Table 3, entries 8, 13, 20, and 22) evidenced a good degree of control over the polymerization. The overall good match between calculated (M_n(theor)) and experimental molecular weights (M_n(SEC) and M_n(NMR)) and the narrow molecular weight distributions ranging from 1.09 to 1.11 establish that adequate conditions were met for effective living immortal conditions: i.e., the transfer reaction between dormant hydroxyl-end-capped polymer chains and the active alkoxy-type polymer chain coordinated onto the aluminum center proceeded significantly more quickly than propagation.[1h,i] Accordingly, analysis by ^{1}H NMR spectroscopy in $CDCl_3$ of reprecipitated PLAs obtained under such conditions revealed the presence of an isopropoxycarbonyl moiety (doublets at δ 1.25 ppm for the methyl groups and a multiplet at δ 5.10 ppm for the methine hydrogen, which mostly overlapped with the PLA signals) or a benzyloxycarbonyl moiety (multiplets at δ 7.30 ppm for the aromatics and a resonance that is overlapped with the PLA signal) at one

dx.doi.org/10.1021/om301155m | *Organometallics* XXXX, XXX, XXX–XXX

Table 3. (*i*)ROP of *rac*-Lactide Promoted by Catalytic Systems Made of Aluminum Complexes 1a−m and an Exogenous Alcohol

entry	[Al]	ROH	[LA]/[Al]/[ROH][a]	time[b] (h)	conversn[c] (%)	M_n(theor)[d] (g.mol^{-1}) (× 10^3)	M_n(NMR)[e] (g.mol^{-1}) (× 10^3)	M_n(SEC)[f] (g.mol^{-1}) (× 10^3)	M_w/M_n[f]	P_m[g]
1	**1a**	BnOH	100/1/1	15	69	9.7	nd	4.8	1.10	0.30
2	**1a**	*i*PrOH	100/1/1	17	66	9.2	7.6	5.7	1.12	0.29
3	**1a**	BnOH	100/1/2	20	85	6.1	nd	4.1	1.12	0.32
4	**1b**	*i*PrOH	100/1/1	16	82	11.8	8.7	9.4	1.13	0.50
5	**1c**	BnOH	100/1/1	17	88	12.8	nd	10.4	1.17	0.65
6	**1d**	*i*PrOH	100/1/1	16	90	13.0	7.8	10.1	1.21	0.56
7	**1e**	BnOH	100/1/1	16	78	11.2	nd	8.0	1.14	0.50
8	**1e**	*i*PrOH	1000/1/10	18	61	8.8	7.2	5.8	1.09	nd
9	**1f**	*i*PrOH	100:1:1	2	27	3.9	4.2	3.4	1.11	0.70
10	**1f**	*i*PrOH	100/1/1	4	39	5.6	5.5	5.5	1.08	0.67
11	**1f**	*i*PrOH	100/1/1	6	46	6.6	6.8	6.2	1.09	0.73
12[h]	**1f**	BnOH	100/1/1	16	97	14.0	nd	11.9	1.35	1.00[h]
13	**1f**	*i*PrOH	1000/1/10	17	29	4.2	3.6	3.3	1.11	0.63
14	**1g**	*i*PrOH	100/1/1	16	78	11.2	10.1	7.3	1.24	0.50
15	**1h**	*i*PrOH	100/1/1	18	74	10.7	6.7	8.5	1.18	0.76
16	**1i**	*i*PrOH	100/1/1	16	79	11.3	12.9	11.3	1.51	0.80
17	**1j**	*i*PrOH	100/1/1	16	80	11.5	8.1	9.9	1.32	0.71
18	**1k**	*i*PrOH	100/1/1	16	96	13.8	10.8	14.9	1.23	0.42
19	**1l**	BnOH	100/1/1	17	95	13.3	nd	10.8	1.46	0.47
20	**1l**	*i*PrOH	1000/1/10	17	33	4.8	4.0	3.8	1.10	0.46
21	**1m**	BnOH	100/1/1	15	84	12.1	nd	9.0	1.21	0.40
22	**1m**	*i*PrOH	1000/1/10	18	61	8.8	nd	5.7	1.11	0.42
23	**7a**		100/1/0	24	0					
24	**7a**[i]		100/1/0	18	58	4.2	nd	3.2	1.30	0.51

[a]Polymerization conditions unless otherwise stated: reactions performed in slurry/solution, [*rac*-LA]$_0$ = 2.0 M at 100 °C. [b]Reaction times were not necessarily optimized. [c]Monomer conversion determined by ^{1}H NMR spectroscopy ($CDCl_3$, 298 K). [d]Calculated molecular weight calculated using M_n(theor) = conversion × [*rac*-LA]$_0$/[Al or ROH] × M_{LA}. [e]Experimental molecular weight determined by NMR from the relative intensities of the main chain and terminal resonances. [f]Experimental molecular weight determined by SEC vs polystyrene standards and corrected by a factor of 0.58. [g]P_m is the probability of a meso linkage, as determined by homonuclear decoupled ^{1}H NMR experiments. [h]Experiment using L-lactide as the monomer. [i]Experiment run in bulk at 125 °C.

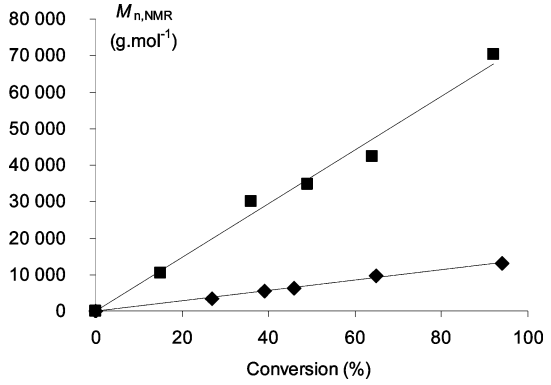

Figure 6. Plot of M_n(NMR) (g mol^{-1}) vs. *rac*-lactide conversion (%) using **1f**/*i*PrOH at [*rac*-LA]$_0$/[Al]/[*i*PrOH]$_0$ ratios of 100/1/1 (◆) and 500/1/1 (■). Both solid lines correspond to the calculated M_n values.

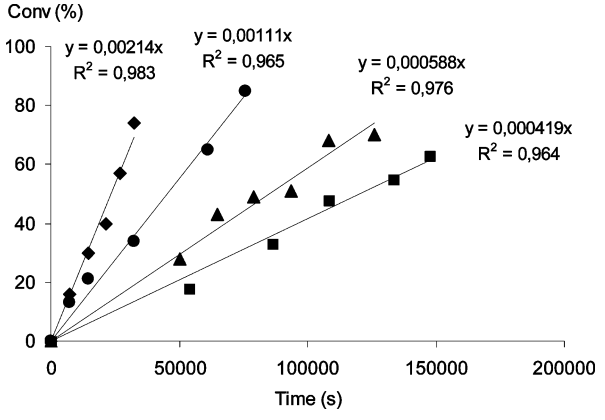

Figure 7. Plot of *rac*-LA conversion (%) vs time (s) with the binary system **1m**/*i*PrOH at [*rac*-LA]$_0$/[Al]/[*i*PrOH]$_0$ = 500/1/5 ([*rac*-LA]$_0$ = 2.0 M) and different temperatures: (■) 90 °C; (▲) 100 °C; (●) 110 °C; (◆) 120 °C.

terminus and of the methine hydrogen in the α-position of the terminal alcohol $CH(OH)CH_3$ (broadened quartet at δ 4.35 ppm) at the other terminus of the polymer chain (see Figure S72, Supporting Information).

The microstructure of the formed PLAs was determined by homonuclear decoupled ^{1}H NMR spectra of the methine region.[30] Interestingly, samples derived from **1a−m** were indicative of the formation of chains with either heterotactic- or isotactic-biased microstructures. In fact, the nature of the imino substituent on the phenoxy-imine ligand significantly affects the ability of the catalyst to control monomer enchainment in the ROP of *rac*-lactide. Polymerization reactions conducted with systems based on {ONN^{qui}}AlMe$_2$ (**1a**), {ON^{trityl}}AlMe$_2$ (**1k**), and {ON^{pipeBn}}AlMe$_2$ (**1m**) led to heterotactic-enriched PLAs (P_m = 0.30−0.42, entries 1−3, 18, 21 and 22) whereas complexes {ON^{ArF}}AlMe$_2$ (**1c**), {ON^{Bn}}AlMe$_2$ (**1f**), {ON^{CH2Mes}}AlMe$_2$ (**1h**), {ON^{PhOMe}}AlMe$_2$ (**1i**), and {ON^{CHPh2}}AlMe$_2$ (**1j**) led to isotactic PLAs (P_m = 0.65−0.80, entries 5, 9−13, and 15−17). In contrast, {ON^{PhiPr2}}-

dx.doi.org/10.1021/om301155m | *Organometallics* XXXX, XXX, XXX−XXX

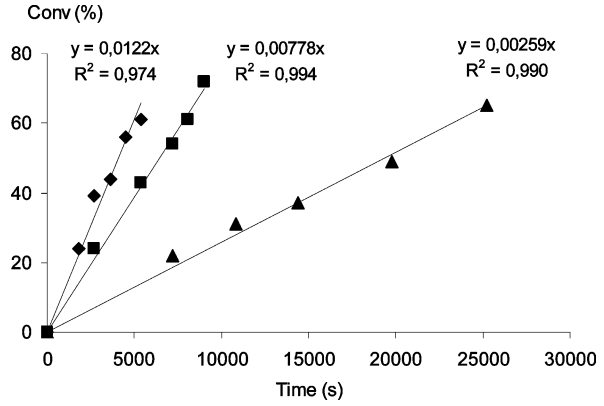

Figure 8. Plot of *rac*-LA conversion (%) vs time (s) at 110 °C with the binary system **1m**/*i*PrOH, with $[rac\text{-LA}]_0$ = 2.0 M and $[i\text{PrOH}]_0$ = 0.10 M, at different concentrations of precatalyst: (▲) [Al] = 4.0 mM; (■) [Al] = 12 mM; (◆) [Al] = 20 mM.

Table 4. Apparent Rate Constants Determined for the ROP of *rac*-Lactide with Binary Systems 1m/*i*PrOH and Single Component 8m[a]

complex	temp (°C)	$[rac\text{-LA}]_0/[\text{Al}]/[i\text{PrOH}]_0$	k_{app} (10^{-3} s^{-1})
1m	90	500/1/5	0.44 ± 0.05
1m	100	500/1/5	0.59 ± 0.04
1m	110	500/1/5	1.1 ± 0.1
1m	120	500/1/5	2.1 ± 0.1
1m	110	500/1/20	2.1 ± 0.3
1m	110	500/1/25	2.6 ± 0.3
1m	110	500/3/25	7.8 ± 0.3
1m	110	500/5/25	12.2 ± 0.9
8m	110	200/1/0	1.4 ± 0.1

[a]All reactions were performed with $[rac\text{-LA}]_0$ = 2.0 M in toluene.

$AlMe_2$ (**1b**), $\{ON^{Phmorpho}\}AlMe_2$ (**1e**), $\{ON^{CH2pyr}\}AlMe_2$ (**1g**), and $\{ON^{MeBu}\}AlMe_2$ (**1l**) (P_m = 0.47−0.56, entries 4, 7, 14 and 19−20) were found to be essentially nonstereoselective.

The trend in isoselectivity toward *rac*-LA can be in part rationalized for some systems having a benzyl-type imino substituent. It seems to follow grossly the bulkiness of the aryl moiety in the benzyl substituent: 3,4,5-trimethoxyphenyl (**i**, P_m = 0.80) > mesityl (**h**, P_m = 0.76) > phenyl (**f**, P_m = 0.63−073). However, bulkiness is apparently not the sole parameter that affects isotacticity in this series of compounds, as demonstrated by the almost identical isoselectivity of the benzyl (**f**, P_m = 0.68 ± 0.05) and benzal moieties (**j**, P_m = 0.71) while the bulkier trityl substituent induced a reversal in stereocontrol, with a slightly heterotactic enriched polymer (**k**, P_m = 0.42, entry 18). Trying to rationalize the heteroselectivity observed for several systems appears even much trickier. The highest value was obtained with the 8-quinolyl substituent (**a**, P_m = 0.30, entries 1−3), and modestly heterotactic-enriched polymers were obtained with the piperidinylbenzyl (**m**, P_m = 0.40−0.42, entries 21 and 22) and trityl moieties (**k**, P_m = 0.42, entry 18). It is noteworthy that bulkiness has no significant effect on the stereoselectivity of systems having a ligand derived from aniline derivatives, as attested by the narrow range of P_m values obtained with quite different substituents on the aryl moiety: 2,6-diisopropyl (**b**, P_m = 0.50), 3,5-bis(trifluoromethyl) (**c**, P_m = 0.65), 2,6-bis(3,5-bis(trifluoromethyl)phenyl) (**d**, P_m = 0.56), and 2-morpholinyl (**e**, P_m = 0.50). Similarly, no stereoselectivity was observed for the aluminum complex bearing a chiral alkyl substituent (**l**, P_m = 0.47, entries 19 and 20).

Indium-Based Initiators. The performance of the dimethylindium complexes **2a,m** and of the bis((trimethylsilyl)methyl)-indium complexes **3a,f,g,l,m** was next assessed. Representative results obtained in the (*i*)ROP of *rac*-LA in the presence of exogenous CTAs are reported in Table 5.

Table 5. (*i*)ROP of *rac*-Lactide Promoted by Binary Systems Made of Isopropyl Alcohol and Indium Complexes 2a,m, and 3a,f,g,l,m

entry	[In]	$[LA]/[In]/[i\text{PrOH}]^a$	time[b] (h)	conversn[c] (%)	M_n(theor)[d] ($\times 10^3$ g mol^{-1})	M_n(NMR)[e] ($\times 10^3$ g mol^{-1})	M_n(SEC)[f] ($\times 10^3$ g mol^{-1})	M_w/M_n[f]	P_m[g]
1	**2a**	100/1/1	3	86	12.4	13.0	9.9	1.58	0.50
2	**2a**	100/1/1	2.5	98	14.1	13.5	13.4	1.45	0.49
3	**2a**	100/1/2	24	99	7.2	6.6	4.4	1.96	nd
4	**2a**	500/1/1	3	56	40.3	13.8	14.5	1.38	0.52
5	**2a**	500/1/1	16	93	67.0	33.0	26.6	1.90	nd
6	**2m**	100/1/1	2	90	12.9	10.1	9.0	1.33	nd
7	**2m**	100/1/1	17	99	14.4	13.7	7.3	1.69	nd
8	**2m**	100/1/1	0.25	93	13.4	14.2	9.1	1.80	nd
9	**2m**	100/1/1	0.5	99	14.4	nd	7.2	1.53	nd
10	**2m**	500/1/1	16	97	70.0	40.0	27.6	1.91	0.47
11	**2m**	1000/1/10	15	98	14.1	12.2	11.8	1.60	0.48
12[h]	**3a**	1000/1/10	18	97	14.0	13.3	13.7	1.12	0.70
13	**3f**	1000/1/10	16	87	12.5	11.1	9.5	1.13	0.44
14	**3g**	1000/1/10	19	91	13.1	14.6	14.4	1.08	0.54
15	**3h**	1000/1/10	16	87	12.5	9.7	13.3	1.07	0.44
16	**3l**	1000/1/10	15	86	12.4	14.5	12.8	1.10	0.46
17	**3m**	1000/1/10	3	67	9.7	7.9	6.8	1.06	0.52

[a]Polymerization conditions unless otherwise stated: $[rac\text{-LA}]_0$ = 2.0 M at 80 °C. [b]Reaction times were not necessarily optimized. [c]Monomer conversion determined by ^{1}H NMR spectroscopy ($CDCl_3$, 298 K). [d]Theoretical molecular weight calculated using M_n(theor) = conversion × $[rac\text{-LA}]_0/[\text{In or iPrOH}]$ × M_{LA}. [e]Experimental molecular weight determined by NMR from the relative intensities of the main chain and terminal resonances; due to the important uncertainty in relative intensities for high degrees of polymerization, values above 15000 g mol^{-1} must be seen as estimates. [f]Experimental molecular weight determined by SEC vs polystyrene standards and corrected by a factor of 0.58. [g]P_m is the probability of meso linkages, as determined by homonuclear decoupled ^{1}H NMR experiments. [h]This experiment was duplicated.

dx.doi.org/10.1021/om301155m | *Organometallics* XXXX, XXX, XXX−XXX

Complexes {ONN^{qui}}InMe$_2$ (**2a**) and {ON^{pipeBn}}InMe$_2$ (**2m**), on combination with 1−2 equiv of isopropyl alcohol, showed interesting performance in the ROP of *rac*-LA in toluene solution at 80 °C. Under these conditions, non-optimized turnover frequencies determined from these batch experiments reached up to 37 mol of LA (mol of In)$^{-1}$ h^{-1}. These apparent TOF values[27] are greater than those of their aluminum counterparts (especially considering that the latter were achieved at a higher temperature: i.e., 100 °C) but somewhat lower than those found for the dinuclear halide-/ethoxy-bridged indium complex reported by Mehrkhodavandi et al.[24] (50 mol of LA (mol of In)$^{-1}$ h^{-1} at 25 °C) or the dinuclear isopropoxy-bridged indium complex described by Okuda et al.[31] (49 mol of LA (mol of In)$^{-1}$ h^{-1} at 50 °C). All the PLAs formed under those conditions had unimodal, although broadened, molecular distributions (M_w/M_n = 1.33−1.96) and experimental molecular weights determined by SEC quite close to the theoretical values calculated on the assumption of the growth of one macromolecular chain per added alcohol equivalent (see Figure S73, Supporting Information). A noticeable deviation from this trend occurred when the monomer loading was increased from 100 to 500 equiv (Table 5, entries 4, 5, and 10), which led to PLAs with molecular weights significantly lower than those expected, demonstrating a rather low degree of control over the polymerization provided by these systems, in contrast to what could be achieved by their aluminum congeners (vide supra). We assume that this may reflect the occurrence of transfer to the monomer and/or transesterification side reactions under such conditions, as supported by the rather broad dispersity values. On the other hand, carrying out the polymerization in the presence of a larger excess (10 equiv) of CTA (entry 11) afforded polymers with experimental molecular weights (M_n(SEC) and M_n(NMR)) that matched well with the theoretical M_n values and with narrow polydispersity indexes.

The bis((trimethylsilyl)methyl)indium complexes **3a,f,g,l,m** were tested with an excess of alcohol in the ROP of *rac*-LA at a monomer/catalyst/initiator alcohol ratio of 1000/1/10. All the systems exhibited good control over the polymerization parameters with fast and efficient transfer between the growing polymer chains and the dormant (macro)alcohols, as evidenced by the narrow molecular weight distribution of the resulting polymers (M_w/M_n = 1.06−1.13)[32] and the agreement between theoretical and observed molecular weights. ^{1}H NMR spectroscopy of a rather low molecular weight PLA established that it is selectively capped by isopropoxycarbonyl and hydroxyl end groups.

Kinetics of the ROP of *rac*-LA with the **3m**/*i*PrOH system were determined under conditions identical with those used for the analogous aluminum **1m**/*i*PrOH system (110 °C, [*rac*-LA] = 2.0 M). In contrast to the latter aluminum system, all reactions performed with the indium system featured a more usual first-order dependence on lactide, as evidenced by linear semilogarithmic plots (Figures S81−S86, Supporting Information). Further experiments were conducted with variable amounts of catalyst precursor[33] and alcohol, to determine the corresponding orders in these two components. The apparent rate constants thus determined are reported in Table 6. The experimental gradient of the least-squares fitted line between ln k_{app} vs ln [In] was 0.90(4) (R^2 = 0.934) (Figures S81−S83), indicating a first-order dependence on catalyst concentration. The same treatment for the isopropyl alcohol concentration led to a gradient of 0.28(3) (R^2 = 0.979) (Figures S84−S86),

Table 6. Apparent Rate Constants Determined for the ROP of *rac*-Lactide with Binary Systems 3m/*i*PrOH[a]

$[rac\text{-LA}]_0/[\text{In}]/[i\text{PrOH}]_0$	k_{app} (10^{-3} M^{-1} s^{-1})
500/1/5	0.91 ± 0.10
500/1/10	0.68 ± 0.10
500/1/25	1.1 ± 0.2
500/2/10	1.0 ± 0.3
500/3/10	1.84 ± 0.3

[a]All reactions were performed at 110 °C with $[rac\text{-LA}]_0$ = 2.0 M in toluene.

reflecting the very small different rate constants observed at different alcohol concentrations (vide supra). Thus, for the **3m**/*i*PrOH system, we propose the idealized rate expression $-\text{d}[rac\text{-LA}]/\text{d}t = k_{app}[\text{LA}]^1[\text{In}]^1[i\text{PrOH}]^0$.

Those kinetic differences between the aluminum and indium systems, that is, in the former case an apparent zero-order dependence on monomer and in the latter case a first-order dependence on monomer, were unexpected. Note that this change does not necessarily imply a change in the operative mechanism but could simply reflect a change in the rate-determining step. In fact, the rate law determined for the **3m**/*i*PrOH system can be well accounted for by both coordination−insertion and activated monomer mechanisms. In the coordination−insertion mechanism, the first-order dependence on monomer *and* catalyst classically reflects slow internal nucleophilic attack of the alkoxide (metal-bound) onto the coordinated monomer, and the zero-order dependence on alcohol accounts for fast exchange between active (alkoxide) and dormant (alcohol) polymer chains, as usual for effective immortal systems. On the other hand, in the latter activated monomer mechanism, this first-order dependence on monomer *and* catalyst can be accounted for slow activation (coordination) of the monomer, with rapid attack of the external nucleophile, reflecting the pseudo zero-order dependence on alcohol. More decisive information for identifying the probable mechanism at work comes, in our opinion, from the nonreactivity of dicarbylindium complexes with alcohols under conditions similar to or more drastic than those used in polymerizations and still the controlled formation of alcohol end-capped polymers.

In order to get insights into the reactivity of the dialkyl complexes *under the polymerization conditions*, we first monitored by NMR spectroscopy the reaction of dimethylaluminum complex **1m** with 2 equiv of *i*PrOH and 2.6 equiv of *rac*-LA in C_6D_6. No reaction took place at room temperature as judged by ^{1}H NMR spectroscopy, whereas conversion of the reagents was complete within 16 h at 100 °C, concomitant with release of methane and formation of the corresponding bis(polylactidyl)Al species (Figure S87, Supporting Information). The complexity of the methine resonances of the opened lactide units and the presence of four different C═O moieties in the ^{1}H−^{13}C HMBC NMR spectrum for that species (Figure S88, Supporting Information) evidenced the formation of diastereomeric products. These data are consistent with formation of a major species in which two isopropyl-terminated short chains, derived from two ring-opened lactide units, are bonded to the aluminum center. Most importantly, under strictly identical conditions, indium complex **3m** was found *not* to react with *i*PrOH/*rac*-LA, as judged by NMR spectroscopy. Overall, these observations provide strong clues for supporting

dx.doi.org/10.1021/om301155m | *Organometallics* XXXX, XXX, XXX−XXX

an activated monomer mechanism for the indium-based system, in contrast to aluminum-based systems.

In addition, homodecoupled ^{1}H NMR experiments conducted on PLAs produced with these indium compounds indicated that most of them lead to atactic polymers ($0.44 < P_m < 0.54$); only a modest enrichment in isotactic sequences ($P_m = 0.70$) was achieved with the complex {ONN^{qui}}In(CH$_2$SiMe$_3$)$_2$ (**3a**).[30] This latter value is in contrast with the observed heteroselectivity obtained with the aluminum congener {ONN^{qui}}AlMe$_2$ (**1a**; $P_m = 0.30$). On the other hand, no stereoselectivity was observed for the analogous complex {ONN^{CH2pyr}}In(CH$_2$SiMe$_3$)$_2$ (**3g**; $P_m = 0.54$). Because the fate of these alkyl{phenoxy-imine}metal complexes in the presence of isopropyl alcohol has been shown to be strikingly different—formation of MPV imine reduction products **8a** and **9a** for **1a** and **3a,** respectively, vs no reaction between alcohol and **3g**—and because this fate remains unknown in the presence of lactide (i.e., under the polymerization conditions), it is difficult at this stage to discuss possible reasons for these differences in stereoselectivity. On the other hand, assuming that both **2a** and **3a** polymerize *rac*-LA via an activated monomer mechanism, it can be speculated that the significant difference in stereoselectivity ($P_m = 0.50$ and 0.70, respectively) may arise from the higher steric hindrance induced at the metal center by the CH$_2$SiMe$_3$ moieties as compared to the methyl ones.

CONCLUSIONS

Living (*immortal*) ring-opening polymerization of *rac*-LA was assessed with a variety of dialkyl{phenoxy-imine}aluminum and -indium complexes in combination with an alcohol (*i*PrOH, BnOH) as coinitiator. The dimethylaluminum and dicarbylindium complexes polymerized *rac*-LA in a controlled fashion, while dimethylindium complexes were found to produce PLA with somewhat broad molecular weight distributions and moderate control over the polymerization parameters.

Interestingly, dimethylaluminum complexes having benzyl-type imino substituents enabled the achievement of significant isotacticity (P_m up to 0.80), and the stereocontrol within this series followed grossly the bulkiness of the aryl moiety. Except for the dicarbylindium complex **3a** ($P_m = 0.70$), no indium complexes induced stereoselectivity for the ROP of *rac*-LA. This behavior may be tentatively attributed to the lower steric hindrance induced by the ligand around the indium metallic center in comparison to the aluminum congener, as a result of the larger size of the indium center.[15] However, changes in operative mechanisms from Al to In systems might be another possible explanation.

In fact, kinetic studies revealed different rate laws for two analogous aluminum and indium systems; however, these studies were inconclusive for discerning unambiguously between different operative mechanisms or different rate-determining steps of a given mechanism. On the basis of stoichiometric reactivity studies, we propose that aluminum-based systems operate through a coordination−insertion mechanism, as demonstrated by the similar performances of dimethylaluminum complexes in combination with *i*PrOH in comparison to the isolated bis(isopropyl (*S*)-lactate)aluminum complexes in the ROP of *rac*-LA. On the other hand, we suggest that ROP with these indium-based systems proceeds through an activated monomer mechanism, as supported by the absence of reaction between dialkylindium complexes with exogenous alcohol and still the formation of alcohol-capped PLAs.

EXPERIMENTAL SECTION

General Considerations. All manipulations were performed under a purified argon atmosphere using standard Schlenk techniques or in a glovebox. Solvents were distilled from Na/benzophenone (THF, Et$_2$O) or Na/K alloy (toluene, hexane, and pentane) under argon, degassed thoroughly, and stored under argon prior to use. Deuterated solvents were stored over Na/K alloy (benzene-d_6, toluene-d_8, THF-d_8; >99.5% D, Eurisotop) or CaH$_2$ (CD$_2$Cl$_2$) and vacuum-transferred just before use. CDCl$_3$ was dried over a mixture of 3 and 4 Å molecular sieves. 4-Methyl-6-(triphenylsilyl)-salicylaldehyde,[34] proligands {ONN^{qui}}H,[19] {ON^{Bn}}H,[25] and {ON^{CH2pyr}}H,[25] precursors In(CH$_2$SiMe$_3$)$_3$,[35] In{N(SiMe$_3$)$_2$}$_3$,[36] and In(O*i*Pr)$_3$[37] (also purchased from Alfa Aesar), and complexes {ONN^{qui}}AlMe$_2$ (**1a**),[25] {ON^{Bn}}AlMe$_2$ (**1f**),[25] {ONN^{CH2pyr}}AlMe$_2$ (**1g**),[25] {ONN^{qui}}InMe$_2$ (**2a**),[25] and {ONN^{qui}}In(CH$_2$SiMe$_3$)$_2$ (**3a**)[25] were prepared using literature procedures. *rac*-Lactide (*rac*-LA) was received from Aldrich, and L-lactide (L-LA) was kindly provided by Total Petrochemicals. Purification of either *rac*-LA or L-LA required a three-step procedure involving first a recrystallization from a hot, concentrated *i*PrOH solution (80 °C), followed by two subsequent recrystallizations in hot toluene (100 °C). After purification, *rac*-LA and L-LA were stored at a temperature of −30 °C in the glovebox.

Instrumentation and Measurements. NMR spectra of complexes were recorded on Bruker AC-200, AC-300, Avance DRX 400, and AM-500 spectrometers in Teflon-valved NMR tubes at 25 °C unless otherwise indicated. ^{1}H and ^{13}C NMR chemical shifts are reported in ppm vs SiMe$_4$ and were determined by reference to the residual solvent peaks. Assignment of resonances for organometallic complexes was made from 2D ^{1}H−^{13}C HMQC and HMBC NMR experiments. ^{19}F chemical shifts were determined (when relevant) by external reference to an aqueous solution of NaBF$_4$.

Elemental analyses (C, H, N) were performed using a Flash EA1112 CHNS Thermo Electron apparatus and are the average of two independent determinations.

Size exclusion chromatography (SEC) analyses of PLAs were performed in THF (1.0 mL min^{-1}) at 20 °C using a Polymer Laboratories PL-GPC 50 plus apparatus equipped with two ResiPore 300 × 7.5 mm columns and RI and dual-angle LS (PL-LS 45/90) detectors. The number-average molecular masses (M_n) and polydispersity indexes (M_w/M_n) of the polymers were calculated with reference to a universal calibration vs polystyrene standards. Reported experimental SEC molar mass values (M_n(SEC)) for PLA samples were corrected by a factor of 0.58, as previously established.[38] Unless otherwise stated, the SEC traces of the polymers all exhibited a unimodal, and usually symmetrical, peak.

{ON$^{Ph(iPr)2}$}H (b). A solution of 2-hydroxy-5-methyl-3-(triphenylsilyl)benzaldehyde (1.01 g, 2.56 mmol), 2,6-diisopropylaniline (0.543 g, 3.07 mmol), and PTSA (cat., *ca.* 2.0 mg) in benzene (20 mL) was stirred in a Dean−Stark apparatus at reflux at 110 °C for 48 h. The reaction mixture was cooled to room temperature, and volatiles were removed under vacuum. The resulting solid residue was then recrystallized in methanol at −30 °C to give {ONN$^{Ph(iPr)2}$}H (**b**) as a yellow solid (0.581 g, 41%). ^{1}H NMR (400 MHz, C$_6$D$_6$, 298 K): δ 1.02 (d, $^3J_{H-H}$ = 6.8 Hz, 12H, CH(C*H*$_3$)$_2$), 1.94 (s, 3H, ArC*H*$_3$), 2.90 (q, $^3J_{H-H}$ = 6.7 Hz, 2H, C*H*(CH$_3$)$_2$), 6.86 (s, 1H, H arom), 7.06 (s, 4H, H arom), 7.14−7.19 (m, 8H, H arom), 7.48 (s, 1H, H arom), 7.87−7.88 (m, 6H, H arom), 7.96 (s, 1H, ArC*H*═N), 13.60 (s, 1H, ArO*H*). ^{13}C{^{1}H} NMR (100 MHz, C$_6$D$_6$, 298 K): δ 20.14 (ArCH$_3$), 23.32 (CH(CH$_3$)$_2$), 28.43 (CH(CH$_3$)$_2$), 118.12, 123.15, 123.39, 125.67, 129.45, 134.91, 135.12, 136.87, 138.71, 143.33, 146.75, 164.98 (*ipso*-C phenol), 166.96 (ArCH═N). Anal. Calcd for C$_{38}$H$_{39}$NOSi: C, 82.41; H, 7.10; N, 2.53. Found: C, 82.34; H, 7.24; N, 2.44. Mp: 179 °C.

{ON^{ArF}}H (c). A solution of 2-hydroxy-5-methyl-3-(triphenylsilyl)-benzaldehyde (3.00 g, 7.60 mmol), 3,5-bis(trifluoromethyl)aniline

dx.doi.org/10.1021/om301155m | *Organometallics* XXXX, XXX, XXX−XXX

(2.09 g, 9.12 mmol), and formic acid (2 drops of a 98% pure solution) in methanol (50 mL) was stirred at reflux at 70 °C for 18 h. The reaction mixture was cooled to room temperature, and volatiles were removed under vacuum until the appearance of a precipitate. The suspension was then stored at 4 °C for 24 h. The precipitate was filtered off, washed with cold methanol (3 × 20 mL), and dried in vacuo to give {ON^{PhCF3}}H (**c**) as a yellow solid (2.65 g, 58%). ^{1}H NMR (200 MHz, C_6D_6, 298 K): δ 2.01 (s, 3H, ArCH_3), 6.70 (d, J_{H-H} = 1.5 Hz, 1H, H arom), 6.87 (s, 2H, H arom), 7.21−7.25 (m, 9H, H arom), 7.55 (d, J_{H-H} = 2.7 Hz, 3H, H arom), 7.91−7.93 (m, 6H, H arom and ArC*H*=N), 12.66 (s, 1H, ArO*H*). ^{19}F{^{1}H} NMR (376 MHz, C_6D_6, 298 K): δ − 62.49 (s, 2 CF_3). ^{13}C{^{1}H} NMR (100 MHz, C_6D_6, 298 K): δ 19.89 (ArCH_3), 117.73, 121.41, 121.44, 121.89, 123.25, 124.61, 129.50, 131.62−132.61 (q, $^1J_{C-F}$ = 33.2 Hz, CF_3), 134.61, 135.51, 136.52, 144.34, 149.91, 164.44 (*ipso*-C phenol), 165.28 (ArCH=N). Anal. Calcd for $C_{34}H_{25}F_6NOSi$: C, 67.43; H, 4.16; N, 2.31. Found: C, 68.01; H, 4.36; N, 2.29. Mp: 197 °C.

{ON^{PhCF3}}H (d). This product was prepared as described above for **c** starting from 2-hydroxy-5-methyl-3-(triphenylsilyl)benzaldehyde (0.636 g, 1.61 mmol), 3,3″,5,5″-tetrakis(trifluoromethyl)[1,1′:3′,1″-terphenyl]-2′-amine (0.998 g, 1.93 mmol), and formic acid (2 drops of a 98% solution) to give **d** as a yellow solid (0.342 g, 26%). ^{1}H NMR (400 MHz, C_6D_6, 298 K): δ 1.65 (s, 1H, ArCH_3), 6.34 (d, J_{H-H} = 1.4 Hz, 1H, H arom), 6.85 (d, J_{H-H} = 1.5 Hz, 1H, H arom), 6.86 (s, 1H, H arom), 6.90−6.94 (m, 1H, H arom), 7.08 (s, 1H, ArC*H*=N), 7.25 (t, J_{H-H} = 3.0 Hz, 8H, H arom), 7.28 (m, 1H, H arom), 7.52 (s, 4H, H arom), 7.65 (s, 2H, H arom), 7.73 (m, 6H, H arom), 11.77 (s, 1H, ArO*H*). ^{19}F{^{1}H} NMR (376 MHz, C_6D_6, 298 K): δ −62.57(s, 4 CF_3). ^{13}C{^{1}H} NMR (100 MHz, C_6D_6, 298 K): δ 19.59 (ArCH_3), 116.62, 120.57 (m, $^2J_{C-F}$ = 3.6 Hz, *C*-CF_3), 121.99, 122.91, 124.70, 125.73, 129.22, 129.99, 130.64, 131.39 (q, $^1J_{C-F}$ = 33 Hz, CF_3), 131.21, 134.29, 134.62, 136.40, 17.91, 144.50, 154.47, 164.25 (*ipso*-C phenol), 170.26 (ArCH=N). Anal. Calcd for $C_{48}H_{31}F_{12}NOSi$: C, 64.50; H, 3.50; N, 1.57. Found: C, 64.49; H, 3.56; N, 1.56. Mp: 230 °C.

{ON^{Phmorpho}}H (e). This product was prepared as described above for **c** starting from 2-hydroxy-5-methyl-3-(triphenylsilyl)benzaldehyde (2.00 g, 5.07 mmol), 2-morpholine-aniline (1.08 g, 6.08 mmol), and formic acid (2 drops of a 98% solution) to give **e** as a yellow solid (1.70 g, 60%). ^{1}H NMR (300 MHz, C_6D_6, 298 K): δ 1.99 (s, 3H, ArCH_3), 2.61 (s, 4H, NCH_2 morpholine), 3.45 (s, 4H, OCH_2 morpholine), 6.67−6.75 (m, 2H, H arom), 6.85 (s, 2H, H arom), 7.14−7.22 (m, 11H, H arom), 7.47 (s, 1H, H arom), 7.89 (s, 5H, H arom), 8.14 (s, 1H, ArC*H*=N), 14.36 (s, 1H, ArO*H*). ^{13}C{^{1}H} NMR (125 MHz, $CDCl_3$, 298 K): δ 20.51 (ArCH_3), 52.18 (NCH_2 morpholine), 66.93 (OCH_2 morpholine), 118.38, 118.81, 122.34, 123.28, 127.66, 127.72, 129.29, 129.81, 134.71, 135.21, 135.47, 136.44, 142.78, 146.58, 160.95 (Ar*C*H=N), 164.50 (*ipso*-C phenol). Anal. Calcd for $C_{36}H_{34}N_2O_2Si$: C, 77.94; H, 6.18; N, 5.05. Found: C, 77.85; H, 6.17; N, 5.11. Mp: 211 °C. Crystals suitable for X-ray diffraction studies were grown from slow evaporation of a saturated C_6D_6 solution.

{ON^{CH2mes}}H (h). This product was prepared as described above for **c** starting from 2-hydroxy-5-methyl-3-(triphenylsilyl)benzaldehyde (0.701 g, 1.77 mmol), 2,4,6-trimethylbenzylamine (0.318 g, 2.13 mmol), and formic acid (2 drops of a 98% solution) to give **h** as a yellow solid (0.580 g, 61%). ^{1}H NMR (400 MHz, C_6D_6, 298 K): δ 1.91 (s, 9H, CH_3Mes), 2.09 (s, 3H, ArCH_3), 4.35 (s, 2H, NCH_2Mes), 6.57 (s, 1H, H arom), 6.67 (s, 2H, H aromMes), 7.14−7.16 (m, 8H, H arom), 7.39 (s, 1H, H arom), 7.84−7.89 (m, 7H, H arom and ArC*H*=N), 14.03 (s, 1H, ArO*H*). ^{13}C{^{1}H} NMR (100 MHz, C_6D_6, 298 K): δ 19.27 (*o*-CH_3Mes), 19.97 (*p*-CH_3Ar), 20.63 (*p*-CH_3Ar), 54.60 (NCH_2Mes), 118.31, 121.99, 127.05, 129.08, 129.15, 129.87, 134.21, 135.21, 136.65, 136.93, 137.35, 141.92, 163.52 (ArCH=N), 165.55 (*ipso*-C phenol). Anal. Calcd for $C_{36}H_{35}NOSi$: C, 82.44; H, 6.71; N, 2.66. Found: C, 82.56; H, 6.61; N, 2.68. Mp: 210 °C.

{ON^{BnOMe3}}H (i). This product was prepared as described above for **c** starting from 2-hydroxy-5-methyl-3-(triphenylsilyl)benzaldehyde (1.00 g, 2.53 mmol), 3,4,5-trimethoxybenzylamine (0.600 g, 3.04 mmol), and formic acid (2 drops of a 98% solution) to give **i** as a yellow solid (0.536 g, 37%). ^{1}H NMR (400 MHz, C_6D_6, 298 K): δ 1.98 (s, 3H, ArCH_3), 3.36 (s, 6H, *m*-OCH_3), 3.84 (s, 3H, *p*-OCH_3), 4.21 (s, 2H, NCH_2Ar), 6.28 (s, 2H, H arom), 6.78 (s, 1H, H arom), 7.15−7.16 (m, 10H, H arom), 7.44 (s, 1H, H arom), 7.88−7.89 (m, 7H, H arom and ArC*H*=N), 13.99 (s, 1H, ArO*H*). ^{13}C{^{1}H} NMR (100 MHz, C_6D_6, 298 K): δ 20.01 (ArCH_3), 55.50 (*m*-OCH_3), 60.13 (*p*-OCH_3), 62.22 (NCH_2Ar), 105.28, 118.05, 122.32, 129.19, 133.11, 134.14, 135.10, 136.60, 142.16, 153.98, 164.60 (ArCH=N), 165.21 (*ipso*-C phenol). Anal. Calcd for $C_{36}H_{35}NO_4Si$: C, 75.36; H, 6.15; N, 2.44. Found: C, 75.28; H, 6.13; N, 2.39. Mp: 189 °C.

{ON^{CHPh2}}H (j). This product was prepared as described above for **c** starting from 2-hydroxy-5-methyl-3-(triphenylsilyl)benzaldehyde (0.542 g, 1.37 mmol), benzhydrylamine (0.302 g, 1.65 mmol), and formic acid (2 drops of a 98% solution) to give **j** as a yellow solid (0.210 g, 27%). ^{1}H NMR (400 MHz, C_6D_6, 298 K): δ 1.93 (s, 3H, ArCH_3), 5.20 (s, 1H, NC*H*Ph_2), 6.67 (s, 1H, H arom), 7.01−7.05 (m, 10H, H arom), 7.13−7.16 (m, 9H, H arom), 7.40 (s, 1H, H arom), 7.85−7.90 (m, 7H, H arom and ArC*H*=N), 13.87 (s, 1H, ArO*H*). ^{13}C{^{1}H} NMR (100 MHz, C_6D_6, 298 K): δ 19.98 (ArCH_3), 76.27 (NCHPh_2), 118.13, 122.17, 127.08, 128.50, 129.21, 134.56, 135.08, 136.64, 142.41, 142.56, 164.54 (*ipso*-C phenol), 165.18 (ArCH=N). Anal. Calcd for $C_{39}H_{33}NOSi$: C, 83.68; H, 5.87; N, 2.20. Found: C, 83.69; H, 5.85; N, 2.22. Mp: 176 °C.

{ON^{trityl}}H (k). This product was prepared as described above for **c** starting from 2-hydroxy-5-methyl-3-(triphenylsilyl)benzaldehyde (0.500 g, 1.27 mmol), tritylamine (0.394 g, 1.52 mmol), and formic acid (2 drops of a 98% solution) to give **k** as a yellow solid (0.310 g, 38%). ^{1}H NMR (300 MHz, C_6D_6, 298 K): δ 1.86 (s, 3H, ArCH_3), 6.65 (s, 1H, H arom), 6.97−6.99 (m, 9H, H arom), 7.10−7.18 (m, 16H, H arom), 7.42 (d, J_{H-H} = 1.4 Hz, 1H, H arom), 7.88−7.92 (m, 5H, H arom), 8.00 (s, 1H, ArC*H*=N), 14.48 (s, 1H, ArO*H*). ^{13}C{^{1}H} NMR (100 MHz, C_6D_6, 298 K): δ 19.89 (ArCH_3), 79.30 (NCPh_3), 118,16, 122.19, 127.00, 129.20, 129.75, 135.09, 135.17, 136.48, 136.69, 142.66, 144.68, 164.71 (*ipso*-C phenol), 164.96 (ArCH=N). Anal. Calcd for $C_{45}H_{37}NOSi$: C, 85.00; H, 5.87; N, 2.20. Found: C, 85.06; H, 5.97; N, 2.09. Mp: 210 °C.

{ON^{CMetBu}}H (l). This product was prepared as described above for **c** starting from 2-hydroxy-5-methyl-3-(triphenylsilyl)benzaldehyde (3.00 g, 7.60 mmol), (*R*)-3,3-dimethyl-2-butylanine (0.923 g, 9.12 mmol), and formic acid (2 drops of a 98% solution) to give **l** as a yellow solid (1.88 g, 52%). ^{1}H NMR (400 MHz, C_6D_6, 298 K): δ 0.68 (s, 9H, C(CH_3)$_3$), 0.81 (d, $^3J_{H-H}$ = 6.4 Hz, 3H, NCHCH_3), 2.02 (s, 3H, ArCH_3), 2.55 (q, $^3J_{H-H}$ = 6.0 Hz, 1H, NC*H*CH$_3$), 6.87 (d, J_{H-H} = 1.5 Hz, 1H, H arom), 7.17−7.19 (m, 9H, H arom), 7.43 (d, J_{H-H} = 1.5 Hz, 1H, H arom), 7.86 (s, 1H, ArC*H*=N), 7.88−7.90 (m, 5H, H arom), 13.92 (s, 1H, ArO*H*). ^{13}C{^{1}H} NMR (100 MHz, C_6D_6, 298 K): δ 16.93 (NCHCH$_3$), 20.05 (ArCH_3), 26.10 (C-(CH_3)$_3$), 33.61 (*C*(CH_3)$_3$), 74.23 (NCHCH$_3$), 118.04, 122.04, 127.06, 129.15, 134.01, 135.20, 136.64, 141.90, 162.95 (ArCH=N), 164.74 (*ipso*-C phenol). Anal. Calcd for $C_{32}H_{35}NOSi$: C, 80.46; H, 7.38; N, 2.93. Found: C, 80.59; H, 7.08; N, 2.95. Mp: 165 °C. Crystals suitable for X-ray diffraction studies were grown from slow evaporation of a saturated C_6D_6 solution.

{ON^{pipeBn}}H (m). This product was prepared as described above for **b** starting from 2-hydroxy-5-methyl-3-(triphenylsilyl)benzaldehyde (2.00 g, 5.07 mmol), 4-amino-1-benzylpiperidine (1.16 g, 6.08 mmol), and formic acid (2 drops of a 98% solution) to give **m** as a yellow solid (1.79 g, 62%). ^{1}H NMR (400 MHz, C_6D_6, 298 K): δ 1.30 (m, 2H, CH_2 pip), 1.46 (qd, J_{H-H} = 10.2 and 3.5 Hz, 2H, CH_2 pip), 1.79 (t, $^3J_{H-H}$ = 10.2 Hz, 2H, CH_2 pip), 2.03 (s, 3H, ArCH_3), 2.57 (m, 2H, CH_2 pip), 2.70 (m, 1H, C*H* pip), 3.26 (s, 2H, NCH_2Ph), 6.87 (d, $^3J_{H-H}$ = 1.5 Hz, 1H, H arom), 7.17−7.25 (m, 10H, H arom), 7.32 (s, 1H, H arom), 7.34 (s, 1H, H arom), 7.45 (d, J_{H-H} = 1.8 Hz, 1H, H arom), 7.83 (s, 1H, ArC*H*=N), 7.90 (m, 6H, H arom), 13.80 (s, 1H, ArO*H*). ^{13}C{^{1}H} NMR (100 MHz, C_6D_6, 298 K): δ 20.09 (ArCH_3), 33.13 (CH_2pip), 51.65 (CH_2pip), 62.79 (NCH_2Ph), 65.41 (C*H* pip), 118.17, 122.18, 126.89, 127.07, 128.17, 128.65, 129.18, 133.93, 135.19, 136.66, 139.28, 141.99, 162.76 (ArCH=N), 164.68 (*ipso*-C phenol). Anal. Calcd for $C_{38}H_{38}N_2OSi$: C, 80.52; H, 6.76; N, 4.94. Found: C, 80.53; H, 6.56; N, 4.81. Mp: 211 °C.

dx.doi.org/10.1021/om301155m | *Organometallics* XXXX, XXX, XXX−XXX

{ON$^{Ph(iPr)2}$}AlMe$_2$ (1b). A solution of {ON$^{Ph(iPr)2}$}H (**b**; 0.096 g, 0.170 mmol) in toluene (2 mL) was added to a solution of AlMe$_3$ (0.170 mL of a 1.0 M solution in *n*-hexane, 0.41 mmol) in toluene (1 mL). The reaction mixture was stirred at room temperature for 18 h. Then, the volatiles were evaporated and the resulting material was washed with *n*-hexane (2 × 1 mL) and dried under vacuum to give **1b** as a yellow solid (0.067 g, 65%). ^{1}H NMR (400 MHz, C_6D_6, 298 K): δ −0.77 (s, 6H, Al(CH_3)$_2$), 0.69 (d, $^3J_{H-H}$ = 6.7 Hz, 6H, CH(CH_3)$_2$), 1.03 (d, $^3J_{H-H}$ = 6.6 Hz, 6H, CH(CH_3)$_2$), 1.72 (s, 3H, ArCH_3), 2.95 (m, $^3J_{H-H}$ = 6.6 Hz, 2H, CH(CH_3)$_2$), 6.50 (s, 1H, H arom), 7.00 (s, 1H, H arom), 7.02 (s, 1H, H arom), 7.06−7.08 (m, 1H, H arom), 7.23 (br s, 9H, H arom), 7.64 (s, 1H, H arom), 7.76 (s, 1H, H arom), 7.87 (m, 6H, H arom and ArCH═N). ^{13}C{^{1}H} NMR (100 MHz, C_6D_6, 298 K): δ −9.71 (Al(CH_3)$_2$), 19.67 (ArCH_3), 22.33 (CH(CH_3)$_2$), 25.59 (CH(CH_3)$_2$), 28.10 (CH(CH_3)$_2$), 117.72, 124.07, 126.66, 129.20, 134.97, 136.63, 136.80, 142.19, 142.33, 148.53, 168.28 (*C*−O−Al), 172.96 (ArCH═N). Anal. Calcd for $C_{40}H_{44}$AlNOSi: C, 78.78; H, 7.27; N, 2.30. Found: C, 78.69; H, 7.33; N, 2.33.

{ON^{ArF}}AlMe$_2$ (1c). This product was prepared as described above for **1b** starting from {ON^{ArF}}H (**c**; 0.300 g, 0.495 mmol) and AlMe$_3$ (0.248 mL of a 2.0 M solution in *n*-hexane, 0.495 mmol) to give **1c** as a pale yellow solid (0.200 g, 62%). ^{1}H NMR (300 MHz, C_6D_6, 298 K): δ −0.63 (s, 6H, Al(CH_3)$_2$), 1.93 (s, 3H, ArCH_3), 6.46 (s, 1H, H arom), 7.06 (s, 1H, H arom), 7.25−7.26 (m, 7H, H arom), 7.30 (br s, 1H, H arom), 7.54 (s, 1H, H arom), 7.64 (s, 1H, H arom), 7.83 (m, 6H, H arom and ArCH═N). ^{19}F{^{1}H} NMR (188 MHz, C_6D_6, 298 K): δ −63.16 (s, 2 CF_3). ^{13}C{^{1}H} NMR (125 MHz, C_6D_6, 298 K): δ −9.45 (Al(CH_3)$_2$, 19.62 (ArCH_3), 117.99, 120.87, 120.90, 122.51, 123.89, 126.94, 129.40, 132.81−133.36 (q, $^1J_{C-F}$ = 33.8 Hz, CF_3), 134.66, 136.46, 137.61, 147.86, 149.83. 168.55 (*C*−O−Al), 170.66 (ArCH═N). Anal. Calcd for $C_{36}H_{30}AlF_6NOSi$: C, 65.35; H, 4.57; N, 2.12. Found: C, 65.33; H, 4.58; N, 2.12.

{ON^{PhCF3}}AlMe$_2$ (1d). This product was prepared as described above for **1b** starting from {ON^{PhCF3}}H (**d**; 0.060 g, 0.060 mmol) and AlMe$_3$ (0.067 mL of a 1.0 M solution in *n*-heptane, 0.067 mmol) to give **1d** as a yellow solid (0.033 g, 52%). ^{1}H NMR (500 MHz, C_6D_6, 298 K): δ −1.58 (s, 6H, Al(CH_3)$_2$), 1.84 (s, 3H, ArCH_3), 6.63 (d, J_{H-H} = 1.75 Hz, 1H, H arom), 6.79 (s, 1H, H arom), 6.81 (s, 1H, H arom), 6.93 (m, 1H, H arom), 7.13−7.15 (m, 13H, H arom), 7.25 (t, J_{H-H} = 3.2 Hz, 1H, H arom), 7.27 (s, 1H, ArCH═N), 7.45 (d, J_{H-H} = 2.3 Hz, 1H, H arom), 7.51 (s, 1H, H arom), 7.53 (s, 3H, H arom), 7.58−7.60 (m, 6H, H arom), 7.71 (m, 3H, H arom). ^{19}F{^{1}H} NMR (376 MHz, C_6D_6, 298 K): δ 62.65 (s, 4 CF_3). ^{13}C{^{1}H} NMR (125 MHz, C_6D_6, 298 K): δ −11.10 (Al(CH_3)$_2$), 19.54 (ArCH_3), 116.28, 121.45, 122.18, 124.35, 126.53, 127.05, 129.14, 129.99, 130.64, 131.20, 131.47, 131.57, 131.73, 132.00, 134.53, 134.59, 134.62, 136.33, 140.91, 142.66, 144.50, 150.26, 168.64 (*C*−O−Al), 175.55 (ArCH═N). Anal. Calcd for $C_{50}H_{36}AlF_{12}NOSi$: C, 63.22; H, 3.82; N, 1.47. Found: C, 63.26; H, 3.81; N, 1.47.

{ON^{Phmorpho}}AlMe$_2$ (1e). This product was prepared as described above for **1b** starting from {ON^{Phmorpho}}H (**e**; 0.300 g, 0.541 mmol) and AlMe$_3$ (0.270 mL of a 2.0 M solution in *n*-hexane, 0.541 mmol) to give **1e** as a yellow solid (0.227 g, 70%). ^{1}H NMR (300 MHz, C_6D_6, 298 K): δ −0.59 (s, 6H, Al(CH_3)$_2$), 1.90 (s, 3H, ArCH_3), 2.57 (t, $^3J_{H-H}$ = 4.2 Hz, 4H, NCH_2morpholine), 3.40 (t, $^3J_{H-H}$ = 4.2 Hz, 4H, OCH_2 morpholine), 6.70−6.71 (m, 2H, H arom), 6.76 (t,J_{H-H} = 7.6 Hz, 1H, H arom), 6.91 (t, J_{H-H}= 7.4 Hz, 1H, H arom), 7.22−7.23 (m, 10H, H arom), 7.58 (d, J_{H-H} = 2.0 Hz, 1H, H arom), 7.83−7.86 (m, 7H, H arom and CH═N). ^{13}C{^{1}H} NMR (125 MHz, C_6D_6, 298 K): δ −9.36 (Al(CH_3)$_2$), 19.72 (ArCH_3), 51.25 (NCH_2 morpholine), 66.43 (OCH_2 morpholine), 118.10, 120.74, 123.92, 124.07, 126.53, 127.97, 128.06, 129.22, 125.09, 136.52, 136.77, 140.62, 145.30, 145.29, 168.19 (*C*−O−Al), 174.00 (ArCH═N). Anal. Calcd for $C_{38}H_{39}AlN_2O_2Si$: C, 74.72; H, 6.44; N, 4.59. Found: C, 74.59; H, 6.39; N, 4.43.

{ON^{CH2mes}}AlMe$_2$ (1h). This product was prepared as described above for **1b** starting from {ON^{CH2mes}}H (**h**; 0.100 g, 0.190 mmol) and AlMe$_3$ (0.190 mL of a 1.0 M solution in *n*-heptane, 0.190 mmol) to give **1h** as a yellow solid (0.092 g, 83%). ^{1}H NMR (500 MHz, C_6D_6, 298 K): δ −0.49 (s, 6H, Al(CH_3)$_2$), 1.73 (s, 3H, ArCH_3), 1.86 (s, 6H, CH_3 Mes), 2.06 (s, 3H, CH_3 Mes), 4.38 (d, J_{H-H} = 1.4 Hz, 2H, CH_2 Mes), 6.29 (d, J_{H-H} = 1.9 Hz, 1H, H arom), 6.67 (s, 2H, H arom Mes), 7.21−7.24 (m, 9H, H arom), 7.41 (t, J_{H-H} = 1.5 Hz, 1H, ArCH═N), 7.48 (d, J_{H-H} = 2.2 Hz, 1H, H arom), 7.84−7.87 (m, 6H, H arom). ^{13}C{^{1}H} NMR (125 MHz, C_6D_6, 298 K): δ −10.51 (Al(CH_3)$_2$), 19.00 (*o*-CH_3 Mes), 19.97 (ArCH_3),20.63 (*p*-CH_3 Mes), 50.91 (NCH_2Mes), 118.15, 125.31, 125.96, 126.06, 129.09, 129.36, 135.35, 136.50, 136.82, 138.33, 138.54, 146.81, 166.73 (ArCH═N), 166.87 (*C*−O−Al). Anal. Calcd for $C_{38}H_{40}$AlNOSi: C, 78.45; H, 6.93; N, 2.41. Found: C, 78.58; H, 6.84; N, 2.48.

{ON^{BnOMe3}}AlMe$_2$ (1i). This product was prepared as described above for **1b** starting from {ON^{BnOMe3}}H (**i**; 0.215 g, 0.374 mmol) and AlMe$_3$ (0.374 mL of a 1.0 M solution in *n*-heptane, 0.374 mmol) to give **1i** as a yellow solid (0.117 g, 50%). ^{1}H NMR (400 MHz, C_6D_6, 298 K): δ −0.63 (s, 6H, Al(CH_3)$_2$), 1.87 (s, 3H, ArCH_3), 3.36 (s, 6H, 2 OCH_3), 3.80 (s, 3H, OCH_3), 4.11 (s, 2H, NCH_2Ar), 6.24 (s, 2H, H−Ar(OMe)$_3$), 6.47 (s, 1H, H arom), 7.23 (s, 9H, H arom), 7.46 (s, 1H, ArCH═N), 7.53 (s, 1H, H arom), 7.85 (m, 6H, H arom). ^{13}C{^{1}H} NMR (100 MHz, C_6D_6, 298 K): δ −9.99 (Al(CH_3)$_2$), 19.67 (ArCH_3), 55.66 (*m*-OCH_3), 59.10 (NCH_2Ar), 60.19 (*p*-OCH_3), 107.06, 117.96, 125.99, 129.13, 129.75, 135.26, 136.57, 136.70, 147.25, 154.25, 167.26 (*C*−O−Al), 170.35 (ArCH═N). Anal. Calcd for $C_{38}H_{40}AlNO_4Si$: C, 72.47; H, 6.40; N, 2.22. Found: C, 72.40; H, 6.34; N, 2.34.

{ON^{CHPh2}}AlMe$_2$ (1j). This product was prepared as described above for **1b** starting from {ON^{CHPh2}}H (**j**; 0.100 g, 0.178 mmol) and AlMe$_3$ (0.180 mL of a 1.0 M solution in *n*-heptane, 0.180 mmol) to give **1j** as a yellow solid (0.068 g, 62%). ^{1}H NMR (500 MHz, C_6D_6, 298 K): δ −0.72 (s, 6H, Al(CH_3)$_2$), 1.80 (s, 3H, ArCH_3), 6.08 (s, 1H, NCHPh$_2$), 6.36 (d, J_{H-H} = 1.1 Hz, 1H, H arom), 6.94 (m, 4H, H arom), 6.99−7.01 (m, 6H, H arom), 7.21−7.22 (m, 9H, H arom), 7.55 (d, J_{H-H} = 2.3 Hz, 1H, H arom), 7.80 (s, 1H, ArCH═N), 7.84−7.86 (m, 6H, H arom). ^{13}C{^{1}H} NMR (125 MHz, C_6D_6, 298 K): δ −9.83 (Al(CH_3)$_2$), 19.60 (ArCH_3), 70.15 (NCHPh$_2$), 117.91, 126.05, 128.72, 129.08, 129.10, 135.20, 136.60, 137.12, 138.03, 147.61, 167.55 (*C*−O−Al), 171.00 (ArCH═N). Anal. Calcd for $C_{41}H_{38}$AlNOSi: C, 79.97; H, 6.22; N, 2.27. Found: C, 80.16; H, 6.51; N, 2.13.

{ON^{trityl}}AlMe$_2$ (1k). This product was prepared as described above for **1b** starting from {ON^{trityl}}H (**k**; 0.100 g, 0.157 mmol) and AlMe$_3$ (0.160 mL of a 1.0 M solution in *n*-heptane, 0.160 mmol) to give **1k** as a yellow solid (0.058 g, 57%). ^{1}H NMR (500 MHz, C_6D_6, 298 K): δ −0.89 (s, 6H, Al(CH_3)$_2$), 1.75 (s, 3H, ArCH_3), 6.26 (s, 1H, H arom), 6.96−6.99 (m, 7H, H arom), 7.17 (s, 4H, H arom), 7.21−7.23 (m, 7H, H arom), 7.31 (m, 6H, H arom), 7.59 (s, 1H, H arom), 7.88 (m, 6H, H arom), 8.11 (s, 1H, ArCH═N). ^{13}C{^{1}H} NMR (100 MHz, C_6D_6, 298 K): −8.03 (Al(CH_3)$_2$), 19.55 (ArCH_3), 81.63 (NCPh$_3$), 117.72, 126.02, 129.13, 129.74, 130.69, 135.09, 136.69, 143.32, 144.68, 146.56, 164.95 (*C*−O−Al), 168.43 (ArCH═N). Anal. Calcd for $C_{47}H_{42}$AlNOSi: C, 81.59; H, 6.12; N, 2.02. Found: C, 81.69; H, 6.32; N, 2.20.

{ON^{CMetBu}}AlMe$_2$ (1l). This product was prepared as described above for **1b** starting from {ON^{CMetBu}}H (**l**; 0.300 g, 0.628 mmol) and AlMe$_3$ (0.314 mL of a 2.0 M solution in *n*-hexane, 0.628 mmol) to give **1l** as a bright yellow solid (0.177 g, 53%). ^{1}H NMR (400 MHz, C_6D_6, 298 K): δ −0.64 (s, 3H, Al(CH_3)), −0.63 (s, 3H, Al(CH_3)), 0.57 (s, 9H, C(CH_3)$_3$), 0.90 (d, $^3J_{H-H}$ = 6.5 Hz, 3H, NCHCH_3), 1.88 (s, 3H, ArCH_3), 2.87 (q, $^3J_{H-H}$ = 6.9 Hz, 1H, NCHCH$_3$), 6.58 (d, J_{H-H} = 2.2 Hz, 1H, H arom), 7.11 (s, 1H, H arom), 7.15−7.16 (m, 8H, H arom), 7.55 (s, 1H, H arom, ArCH═N), 7.87 (m, 6H, H arom). ^{13}C{^{1}H} NMR (100 MHz, C_6D_6, 298 K): δ −8.45 (Al(CH_3)), −8.15 (Al(CH_3)), 15.78 (NCHCH$_3$), 19.76 (ArCH_3), 26.79 (C(CH_3)$_3$), 35.02 (C(CH_3)$_3$), 70.52 (NCHCH$_3$), 117.95, 117.95, 125.93, 129.10, 135.20, 136.63, 136.88, 147.11, 167.47 (*C*−O−Al), 170.60 (ArCH═N). Anal. Calcd for $C_{34}H_{40}$AlNOSi: C, 76.51; H, 7.55; N, 2.62. Found: C, 76.42; H, 7.84; N, 2.43.

{ON^{pipeBn}}AlMe$_2$ (1m). This product was prepared as described above for **1b** starting from {ON^{pipeBn}}H (**m**; 0.300 g, 0.530 mmol) and AlMe$_3$ (0.530 mL of a 1.0 M solution in *n*-heptane, 0.530 mmol) to give **1m** as a yellow solid (0.208 g, 63%). ^{1}H NMR (500 MHz, C_6D_6, 298 K): δ −0.55 (s, 6H, Al(CH_3)$_2$), 1.37 (m, 2H, CH_2 pip), 1.55 (td,

dx.doi.org/10.1021/om301155m | *Organometallics* XXXX, XXX, XXX−XXX

J_{H-H} = 10 and 2.0 Hz, 2H, CH_2 pip), 1.72 (qd, J_{H-H} = 8.6 and 3.6 Hz, 2H, CH_2 pip), 1.96 (s, 3H, ArCH_3), 2.62 (m, 2H, CH_2 pip), 2.80 (m, 1H, NCH(CH_2)$_2$), 3.23 (s, 2H, NCH_2Ph), 6.56 (d, J_{H-H} = 1.8 Hz, 1H, H arom), 7.05−7.29 (m, 14H, H arom), 7.38 (s, 1H, ArCH=N), 7.55 (dd, J_{H-H} = 1.9 and 0.5 Hz, 1H, H arom), 7.87 (m, 6H, H arom). $^{13}C\{^1H\}$ NMR (125 MHz, C_6D_6, 298 K): δ −8.45 (Al(CH_3)$_2$), 19.75 (ArCH_3), 32.60 (CH_2 pip), 52.19 (CH_2 pip), 62.56 (NCH_2Ph), 65.59 (NCH), 118.01, 125.79, 127.11, 127.95, 128.28, 128.72, 129.11, 135.25, 136.59, 136.71, 138.58, 147.04, 167.24 (C−O−Al), 168.91 (ArCH=N). Anal. Calcd for $C_{40}H_{43}AlN_2OSi$: C, 77.13; H, 6.96; N, 4.50. Found: C, 76.87; H, 7.06; N, 4.83. Crystals suitable for X-ray diffraction studies were grown from a saturated Et_2O solution layered with hexanes at room temperature.

{ON^{pipeBn}}InMe$_2$ (2m). To a stirred suspension of $InCl_3$ (0.117 g, 0.529 mmol) in Et_2O (ca. 5 mL) was added a solution of MeLi (1.0 mL of a 1.6 M solution in diethyl ether, 1.58 mmol). The reaction mixture was stirred for 30 min at room temperature, and a solution of {ON^{pipeBn}}H (**g**; 0.300 g, 0.529 mmol) in toluene (ca. 5 mL) was added. The resulting reaction mixture was stirred at room temperature for 18 h. Volatiles were removed in vacuo, and the crude product washed with *n*-hexane (ca. 10 mL) to give **2m** as a yellow solid (0.290 g, 77%). ^1H NMR (300 MHz, C_6D_6, 298 K): δ −0.17 (s, 6H, In(CH_3)$_2$), 1.02 (m, 1H, CH_2 pip), 1.59 (m, 3H, CH_2 pip), 1.83 m, 1H, CH_2 pip), 2.59−2.61 (m, 3H, CH_2 pip), 3.24 (s, 2H, NCH_2Ph), 3.29 (m, 1H, CH pip), 6.71 (d, J_{H-H} = 2.2 Hz, 1H, H arom), 7.10−7.18 (m, 8H, H arom), 7.22−7.23 (m, 3H, H arom), 7.41 (s, 1H, H arom), 7.50 (d, J_{H-H} = 2.4 Hz, 1H, H arom), 7.65 (s, 1H, ArCH=N), 7.89−7.91 (m, 8H, H arom). $^{13}C\{^1H\}$ NMR (166 MHz, C_6D_6, 298 K): δ −5.23 (In(CH_3)$_2$), 19.53 (ArCH_3), 33.56 (CH_2 pip), 51.87 (CH_2 pip), 62.61 (NCH_2Ph), 68.95 (CH pip), 117.73, 121.31, 121.87, 123.20, 127.01, 127.18, 127.97, 128.03, 128.30, 128.33, 128.54, 128.80, 129.05, 136.65, 136.68, 136.81, 138.25, 138.57, 146.27, 165.40, 168.88, 172.54 (ArCH=N), 172.97 (ArC−O−In). Anal. Calcd for $C_{40}H_{43}InN_2OSi$: C, 67.60; H, 6.10; N, 3.94. Found: C, 67.34; H, 6.67; N, 3.34. Crystals suitable for X-ray diffraction studies were grown from a saturated Et_2O solution layered with hexanes at room temperature.

{ON^{Bn}}In(CH$_2$SiMe$_3$)$_2$ (3f). A solution of {ON^{Bn}}H (**f**; 0.097 g, 0.201 mmol) in toluene (8 mL) and In(CH_2SiMe_3)$_3$ (0.099 g, 0.201 mmol) in toluene (2 mL) was stirred at 70 °C for 18 h. Then, volatiles were removed in vacuo, *n*-hexane (ca. 10 mL) was vacuum-condensed in, and the resulting solution was filtered off. The filtrate was concentrated under vacuum to give **3f** as a yellow solid (0.077 g, 50%). ^1H NMR (400 MHz, C_6D_6, 298 K): δ −0.72 (d, $^2J_{H-H}$ = 12.6 Hz, 2H, CHHSiMe$_3$), −0.59 (d, $^2J_{H-H}$ = 12.6 Hz, 2H, CHHSiMe$_3$), 0.00 (s, 18H, Si(CH_3)$_3$), 2.03 (s, 3H, ArCH_3), 4.16 (s, 2H, NCH_2Ph), 6.71 (s, 1H, H arom), 6.94 (d, J_{H-H} = 6.9 Hz, 2H, H arom), 7.08−7.10 (m, 4H, H arom), 7.25 (s, 5H, H arom), 7.52 (s, 1H, H arom), 7.55 (s, 1H, ArCH=N), 7.87−7.89 (m, 7H, H arom). $^{13}C\{^1H\}$ NMR (100 MHz, C_6D_6, 298 K): δ −1.35 (CH_2SiMe$_3$), 0.00 (Si(CH_3)$_3$), 17.80 (ArCH_3), 61.65 (NCH_2Ph), 115.81, 121.46, 126.73, 126.89, 127.04, 133.56, 134.29, 134.67, 136.78, 145.02, 168.91 (ArCH=N), 170.70 (ArC−O−In). Anal. Calcd for $C_{41}H_{50}InNOSi_3$: C, 63.79; H, 6.53; N, 1.81. Found: C, 65.94; H, 6.42; N, 1.87.

{ONN^{CH2pyr}}In(CH$_2$SiMe$_3$)$_2$ (3g). This product was prepared as described above for **3f** starting from {ONN^{CH2pyr}}H (**g**; 0.083 g, 0.171 mmol) and In(CH_2SiMe_3)$_3$ (0.085 g, 0.171 mmol) to give **3g** as a bright yellow solid (0.092 g, 70%). ^1H NMR (400 MHz, C_6D_6, 298 K): δ −0.60 (d, $^2J_{H-H}$ = 12.2 Hz, 2H, CHHSiMe$_3$), −0.43 (d, $^2J_{H-H}$ = 12.2 Hz, 2H, CHHSiMe$_3$), 0.08 (s, 18H, Si(CH_3)$_3$), 2.04 (s, 3H, ArCH_3), 4.00 (s, 2H, NCH_2pyr), 6.26 (d, J_{H-H} = 7.7 Hz, 1H, H arom), 6.41 (t, J_{H-H} = 5.7 Hz, 1H, H arom), 6.79−6.81 (m, 2H, H arom), 7.30 (m, 9H, H arom), 7.53 (s, 1H, H arom), 7.61 (s, 1H, ArCH=N), 7.97−8.03 (m, 7H, H arom). $^{13}C\{^1H\}$ NMR (100 MHz, C_6D_6, 298 K): δ −2.09 (CH_2SiMe$_3$), 0.00 (Si(CH_3)$_3$), 17.93 (ArCH_3), 58.82 (NCH_2Ph), 115,34, 119.14, 119.54, 120.76, 126.31, 126.71, 134.63, 134.90, 135.54, 136.21, 144.54, 145.48, 153.21, 169.98 (ArCH=N), 173.50 (ArC−O−In). Anal. Calcd for $C_{40}H_{49}InN_2OSi_3$: C, 62.16; H, 6.39; N, 3.62. Found: C, 62.86; H, 5.97; N, 3.60.

{ON^{CH2mes}}In(CH$_2$SiMe$_3$)$_2$ (3h). This product was prepared as described above for **3f** starting from {ON^{CH2mes}}H (**h**; 0.119 g, 0.226 mmol) and In(CH_2SiMe_3)$_3$ (0.112 g, 0.226 mmol) to give **3h** as a bright yellow solid (0.114 g, 61%). ^1H NMR (400 MHz, C_6D_6, 298 K): δ −0.62 (d, $^2J_{H-H}$ = 12.6 Hz, 2H, CHHSiMe$_3$), −0.53 (d, $^2J_{H-H}$ = 12.6 Hz, 2H, CHHSiMe$_3$), 0.00 (s, 18H, Si(CH_3)$_3$), 1.76 (s, 3H, *p*-CH_3Mes), 1.99 (s, 6H, *o*-CH_3Mes), 2.04 (s, 3H, ArCH_3), 4.33 (s, 2H, NCH_2Ph), 6.49 (s, 1H, H arom), 6.64 (s, 2H, H arom Mes), 7.10−7.15 (s, 8H, H arom), 7.40 (s, 1H, H arom), 7.51 (s, 1H, ArCH=N), 7.87 (m, 7H, H arom). $^{13}C\{^1H\}$ NMR (100 MHz, C_6D_6, 298 K): δ −1.80 (CH_2SiMe_3), 0.00 (Si(CH_3)$_3$), 17.53 (*p*-CH_3 Mes), 17.58 (*o*-CH_3 Mes), 18.58 (ArCH_3), 53.09 (NCH_2Ar), 116.02, 121.42, 126.75, 127.53, 134.26, 134.58, 135.86, 136.31, 136.63, 144.44, 166.21 (ArCH=N), 170.14 (ArC−O−In). Anal. Calcd for $C_{44}H_{56}InNOSi_3$: C, 64.92; H, 6.93; N, 1.72. Found: C, 65.04; H, 6.91; N, 1.66.

{ON^{CMetBu}}In(CH$_2$SiMe$_3$)$_2$ (3l). This product was prepared as described above for **3f** starting from {ON^{CMetBu}}H (**l**; 0.229 g, 0.477 mmol) and In(CH_2SiMe_3)$_3$ (0.236 g, 0.477 mmol) to give **3l** as a bright yellow solid (0.210 g, 57%). ^1H NMR (400 MHz, C_6D_6, 298 K): δ −0.30 (s, 2H, CH_2SiMe$_3$), −0.23 (dd, $^2J_{H-H}$ = 12.6 and 12.5 Hz, 2H, CH_2SiMe$_3$), 0.06 (s, 9H, Si(CH_3)$_3$), 0.13 (s, 9H, Si(CH_3)$_3$), 0.75 (s, 9H, C(CH_3)$_3$), 1.10 (d, 3H, CH(CH_3), 2.06 (s, 3H, ArCH_3), 2.76 (q, $^3J_{H-H}$ = 6.6 Hz, 1H, CH(CH$_3$)), 6.84 (d, J_{H-H} = 2.2 Hz, 1H, H arom), 7.23 (br s, 1H, H arom), 7.26 (d, J_{H-H} = 2.2 Hz, 1H, H arom), 7.29−7.31 (m, 8H, H arom), 7.53 (d, J_{H-H} = 2.4 Hz, 1H, H arom), 7.68 (s, 1H, ArCH=N), 7.89−7.93 (m, 5H, H arom). $^{13}C\{^1H\}$ NMR (125 MHz, C_6D_6, 298 K): δ 2.19 (Si(CH_3)$_3$), 2.32 (Si(CH_3)$_3$), 2.62 (CH_2SiMe$_3$), 2.78 (CH_2SiMe$_3$), 16.38 (CH(CH_3)), 19.83 (ArCH_3), 26.82 (C(CH_3)$_3$), 35.04 (C(CH$_3$)$_3$), 75.47 (CH(CH$_3$)), 118.03, 123.81, 128.95, 129.23, 136.33, 136.72, 139.21, 147.11, 171.67 (ArCH=N), 173.27 (ArC−O−In). Anal. Calcd for $C_{40}H_{56}InNOSi_3$: C, 62.72; H, 7.37; N, 1.83. Found: C, 62.14; H, 7.46; N, 1.84.

{ON^{pipeBn}}In(CH$_2$SiMe$_3$)$_2$ (3m). This product was prepared as described above for **3f** starting from {ON^{pipeBn}}H (**m**; 0.113 g, 0.200 mmol) and In(CH_2SiMe_3)$_3$ (0.098 g, 0.200 mmol) to give **3m** as a bright yellow solid (0.128 g, 75%). ^1H NMR (400 MHz, C_6D_6, 298 K): δ −0.35 (s, 4H, CH_2SiMe$_3$), 0.05 (s, 18H, Si(CH_3)$_3$), 1.43 (m, 2H, CH_2 pip), 1.72 (m, 4H, CH_2 pip), 2.02 (s, 3H, ArCH_3), 2.68 (m, 3H, CH_2 pip and CH), 3.27 (s, 2H, N−CH_2−Ph), 6.72 (d, J_{H-H} = 2.2 Hz, 1H, H arom), 7.10 (m, 1H, H arom), 7.16−7.24 (m, 12H, H arom), 7.29 (s, 1H, H arom), 7.31 (s, 1H, H arom), 7.50 (s, 2H, H arom and ArCH=N), 7.83−7.87 (m, 5H, H arom). $^{13}C\{^1H\}$ NMR (100 MHz, C_6D_6, 298 K): δ −2.52 (CH_2SiMe$_3$), 0.24 (Si(CH_3)$_3$), 17.60 (ArCH_3), 31.52 (CH_2 pip), 49.75 (CH_2 pip), 60.61 (NCH_2Ph), 65.57 (CH pip), 115.86, 121.24, 126.44, 126.67, 127.00, 134.06, 134.47, 136.34, 136.55, 144.63, 167.18 (ArCH=N), 170.65 (ArC−O−Al). Anal. Calcd for $C_{45}H_{56}InN_2OSi_3$: C, 64.34; H, 6.72; N, 3.33. Found: C, 64.15; H, 7.01; N, 3.36.

{ONN^{qui}}Al((1*R*,2*S*,5*R*)-menthyl (*S*)-lactate)$_2$ (7a). THF (ca. 10 mL) was vacuum-condensed in a Schlenk flask containing {ONN^{qui}}AlMe$_2$ (**1a**; 0.200 g, 0.347 mmol) and (1*R*,2*S*,5*R*)-menthyl (*S*)-H-lactacte (0.158 g, 0.694 mmol). The reaction mixture was stirred at room temperature for 30 min. Then, the solvent was evaporated in vacuo, *n*-pentane (ca. 10 mL) was vacuum-condensed in, and the flask was stored at −30 °C for 72 h. The precipitate that formed was filtered off and washed with pentane (ca. 5 mL). The resulting residue was dried under vacuum to give **7a** as an orange solid (0.104 g, 30%). ^1H NMR (400 MHz, C_6D_6, 298 K): δ 0.11 (d, J_{H-H} = 6.6 Hz, 3H, CHCH(CH_3)$_2$), 0.52 (m, 3H, CHCH_3), 0.59 (m, 9H, CHCH(CH_3)$_2$ and CH_2), 0.67 (d, J_{H-H} = 5.7 Hz, 3H, CHCH_3), 0.76 (d, J_{H-H} = 6.8 Hz, 6H, CHCH(CH_3)$_2$ and CH_2), 0.77 (m, 2H, CH_2), 1.05 (m, 2H, CHCH(CH$_3$)$_2$), 1.18 (d, J_{H-H} = 6.6 Hz, 3H, OCHCH_3), 1.29 (m, 8H, CH and CH_2), 1.46 (d, J_{H-H} = 6.5 Hz, 3H, OCHCH_3), 1.96 (s, 3 H, ArCH_3), 4.24 (q, J_{H-H} = 6.9 Hz, 1H, OCHCH$_3$), 4.30 (m, 2H, CHCH$_3$), 4.57 (q, J_{H-H} = 6.9 Hz, 1H, OCHCH$_3$), 6.8 (m, 1H, H arom), 7.00 (m, 1H, H arom), 7.08−7.19 (m, 4H, H arom), 7.29−7.58 (m, 12H, H arom), 8.10 (d, J_{H-H} = 6.4 Hz, 6H, H arom), 8.67 (s, 1H, ArCH=N), 9.20 (s, 1H, H arom). $^{13}C\{^1H\}$ NMR (125 MHz, C_6D_6, 298 K): δ 15.64 (CHCH(CH_3)$_2$), 15.98 (CHCH(CH_3)$_2$), 19.92 (ArCH_3), 20.33 (CHCH(CH_3)$_2$), 20.72 (CHCH(CH_3)$_2$), 21.64

dx.doi.org/10.1021/om301155m | *Organometallics* XXXX, XXX, XXX−XXX

($CHCH_3$), 21.71 ($CHCH_3$), 22.89 ($OCHCH_3$), 23.03 (CH_2), 23.18 ($OCHCH_3$), 23.33 (CH_2), 25.59 ($CHCH(CH_3)_2$), 25.88 ($CHCH(CH_3)_2$), 30.85 (CH_2), 33.91 (CH_2), 34.03 (CH_2), 40.42 (C(O)OCH), 40.64 (C(O)OCH), 46.73 ($CHCH(CH_3)_2$), 46.80 ($CHCH(CH_3)_2$), 68.00 ($OCHCH_3$), 68.47 ($OCHCH_3$), 73.41 ($CHCH_3$), 74.05 ($CHCH_3$), 114.75, 119.16, 122.06, 123.79, 124.00, 126.60, 128.17, 128.40, 139.07, 141.02, 147.74, 149.08, 162.81 (ArCH=N), 173.16 (C−Al−O), 181.10 (C=O), 182.69 (C=O). Anal. Calcd for $C_{61}H_{73}AlN_2O_7Si$: C, 73.17; H, 7.35; N, 2.80. Found: C, 73.42; H, 7.98; N, 2.72.

{ON^{Bn}}Al(*i*Pr (*S*)-lactate)$_2$ (8f). A Young NMR tube was charged with isopropyl (*S*)-H-lactate (0.0098 g, 0.074 mmol) and a solution of {ON^{Bn}}$AlMe_2$ (**1c**; 0.020 g, 0.037 mmol) in toluene (0.5 mL). The reaction mixture was heated to 80 °C for 16 h. Then the volatiles were removed and the product was dried in vacuo to give a colorless solid. NMR indicated full conversion of the reagents to the desired product **8f**. ^{1}H NMR (500 MHz, C_6D_6, 298 K): δ 0.76 (d, $^3J_{H-H}$ = 6.1 Hz, 3H, $OCH(CH_3)_2$), 0.91 (d, $^3J_{H-H}$ = 6.2 Hz, 3H, $OCH(CH_3)_2$), 0.97 (d, $^3J_{H-H}$ = 6.1 Hz, 3H, $OCH(CH_3)_2$), 1.00 (d, $^3J_{H-H}$ = 6.2 Hz, 3H, $OCH(CH_3)_2$), 1.32 (d, $^3J_{H-H}$ = 6.7 Hz, 3H, $AlOCH(CH_3)$), 1.56 (d, $^3J_{H-H}$ = 6.60 Hz, 3H, $AlOCH(CH_3)$), 1.80 (s, 3H, $ArCH_3$), 4.41 (q, $^3J_{H-H}$ = 6.8 Hz, 1H, $AlOCH(CH_3)$), 4.46 (m, 1H, $OCH(CH_3)_2$), 4.63 (q, $^3J_{H-H}$ = 6.9 Hz, 1H, $AlOCH(CH_3)$), 4.72 (m, 1H, $OCH(CH_3)_2$), 5.14 (d, $^2J_{H-H}$ = 15.5 Hz, 1H, NCHHPh), 5.14 (d, $^2J_{H-H}$ = 15.5 Hz, 1H, NCHHPh), 6.30 (m, 1H, H arom), 7.00 (d, J_{H-H} = 7.3 Hz, 2H, H arom), 7.05 (t, J_{H-H} = 7.9 Hz, 2H, H arom), 7.19 (m, 7H, H arom), 7.33 (s, 2H, H arom), 7.38 (m, 2H, H arom), 7.59 (s, 1H, ArCH=N), 7.85 (m, 5H H arom), 7.90 (m, 1H, H arom). ^{13}C{^{1}H} NMR (125 MHz, C_6D_6, 298 K): δ 19.71 ($ArCH_3$), 21.05 ($OCH(CH_3)_2$), 21.11 ($OCH(CH_3)_2$), 21.35 ($OCH(CH_3)_2$), 21.38 ($OCH(CH_3)_2$), 22.18 ($AlOCH(CH_3)$), 22.79 ($AlOCH(CH_3)$), 58.00 (NCH_2Ph), 68.09 ($OCH(CH_3)_2$), 68.32 ($AlOCH(CH_3)$), 68.47 ($AlOCH(CH_3)$), 71.56 ($OCH(CH_3)_2$), 118.84, 125.32, 125.52, 125.59, 128.19, 128.47, 128.76, 128.95, 130.53, 136.30, 136.33, 136.51, 136.59, 136.67, 137.31, 137.51, 145.01, 166.83 (ArC−O−Al), 167.66 (ArCH=N), 170.00 (C=O).

{ON^{pipeBn}}Al(*i*Pr (*S*)-lactate)$_2$ (8m). A Schlenk flask was charged with isopropyl (*S*)-H-lactate (0.029 g, 0.22 mmol) and a solution of {ON^{pipeBn}}$AlMe_2$ (**1m**; 0.070 g, 0.011 mmol) in toluene (ca. 5 mL). The reaction mixture was heated to 100 °C for 16 h. Volatiles were removed, and the solid residue was washed with pentane (ca. 5 mL) and then dried in vacuo to give **8m** as a colorless solid (0.067 g, 71%). ^{1}H NMR (400 MHz, C_6D_6, 298 K): δ 0.73 (d, J_{H-H} = 6.2 Hz, 3H, $OCH(CH_3)_2$), 0.95 (d, J_{H-H} = 5.3 Hz, 6H, $OCH(CH_3)_2$), 1.02 (d, J_{H-H} = 6.1 Hz, 3H, $OCH(CH_3)_2$), 1.26 (d, J_{H-H} = 6.9 Hz, 3H, $AlOCH(CH_3)$), 1.51 (d, J_{H-H} = 6.7 Hz, 3H, $AlOCH(CH_3)$), 1.85 (m, 3H, CH_2 pip), 1.95 (s, 3H, $ArCH_3$), 2.02 (m, 1H, CH_2 pip), 2.23 (m, 1H, CH_2 pip), 2.39 (m, 1H, CH_2 pip), 2.87 (m, 3H, CH_2 and CH pip), 3.29 (s, 2H, NCH_2Ph), 4.23 (m, 1H, $OCH(CH_3)_2$), 4.38 (m, 1H, $AlOCH(CH_3)$), 4.55 (m, 1H, $AlOCH(CH_3)$), 4.73 (m, 1H, $OCH(CH_3)_2$), 6.60 (s, 1H, H arom), 6.99−7.01 (m, 1H, H arom), 7.09−7.12 (m, 2H, H arom), 7.17−7.18 (m, 9H, H arom), 7.32 (s, 1H, H arom), 7.34 (s, 1H, H arom), 7.37 (d, J_{H-H} = 2.0 Hz, 1H, H arom), 7.81−7.83 (m, 7H, H arom and ArCH=N). ^{13}C{^{1}H} NMR (100 MHz, C_6D_6, 298 K): δ 18.76 ($ArCH_3$), 20.00 ($OCH(CH_3)_2$), 20.05 ($OCH(CH_3)_2$), 20.40 ($OCH(CH_3)_2$), 21.15 ($AlOCH(CH_3)$), 21.88 ($AlOCH(CH_3)$), 31.42 (CH_2 pip), 32.28 (CH_2 pip), 52.13 (CH_2 pip), 52.26 (CH_2 pip), 59.37 ($OCH(CH_3)_2$), 61.84 (NCH_2Ph), 65.45 (CH pip), 67.12 ($AlOCH(CH_3)$), 67.30 ($AlOCH(CH_3)$), 117.96, 124.27, 124.47, 124.53, 127.70, 127.81, 127.91, 135.27, 135.34, 135.55, 138.36, 143.90, 164.50 (ArCH=N), 165.74 (ArC−O−Al), 174.02 (C=O). Anal. Calcd for $C_{50}H_{59}AlN_2O_7Si$: C, 70.23; H, 6.95; N, 3.28. Found: C, 71.21; H, 7.04; N, 3.78.

General Procedure for Polymerization of *rac*-Lactide. Polymerizations were conducted as previously described.[14] Monomer (LA) conversions were calculated from ^{1}H NMR spectra of the crude reaction mixtures in $CDCl_3$, from the integration (Int) ratio $Int_{polymer}/[Int_{polymer} + Int_{monomer}]$, using the methyl hydrogen resonances for PLA at δ 1.49 ppm and for LA at δ 1.16 ppm. The microstructures of PLAs were determined by homodecoupling ^{1}H NMR spectroscopy (methine region) at 20 °C in $CDCl_3$ on a Bruker AC-500 spectrometer.

Crystal Structure Determinations. Diffraction data for proligands **e**, **f**, and **l** and complexes **1f,g,m**, **2a,m**, **3a**, and **4h** were collected at 100(2) K using a Bruker APEX CCD diffractometer with graphite-monochromated Mo Kα radiation (λ = 0.71073 Å). A combination of ω and ϕ scans was carried out to obtain at least a unique data set. The crystal structures were solved by direct methods; the remaining atoms were located from difference Fourier synthesis followed by full-matrix least-squares refinement based on F^2 (programs SIR97 and SHELXL-97)[39] with the aid of the WINGX program.[40] In most cases, many hydrogen atoms could be found from the Fourier difference analysis. Other hydrogen atoms were placed at calculated positions and forced to ride on the attached atom. The hydrogen atom contributions were calculated but not refined. All non-hydrogen atoms were refined with anisotropic displacement parameters. The locations of the largest peaks in the final difference Fourier map calculation and the magnitudes of the residual electron densities were of no chemical significance. Crystal data and details of data collection and structure refinement for proligands **e**, **f**, and **l** and complexes **1f,g,m**, **2a,m**, **3a**, and **4h** are summarized in Tables S1−S5 (Supporting Information) and can be obtained as well, free of charge, from the Cambridge Crystallographic Data Centre via www.ccdc.cam.ac.uk/data_request/cif (CCDC 912295−912304).

■ ASSOCIATED CONTENT

Ⓢ Supporting Information

CIF files, figures, and tables giving X-ray crystallographic data for proligands **e**, **f**, and **l** and complexes **1f,g,m**, **2a,m**, **3a**, and **4h**, molecular structures of proligands **e**, **f**, and **l** and complexes **1f**, **2a,m**, and **4h**, ^{1}H and ^{13}C{^{1}H} NMR spectra of the prepared proligands and complexes, representative ^{1}H NMR spectra and SEC traces of polymers, and additional kinetics data. This material is available free of charge via the Internet at http://pubs.acs.org.

■ AUTHOR INFORMATION

Corresponding Author

*Fax: (+33)(0)223-236-939. E-mail: evgueni.kirillov@univ-rennes1.fr (E.K.); jean-francois.carpentier@univ-rennes1.fr (J.-F.C.).

Notes

The authors declare no competing financial interest.

■ ACKNOWLEDGMENTS

This work was supported by the *Ministère de l'Enseignement Supérieur et de la Recherche* (Ph.D. fellowship to M.N.). Dedicated in honor of the 80th birthday of Prof. I. P. Beletskaya.

■ REFERENCES

(1) (a) O'Keefe, B. J.; Hillmyer, M. A.; Tolman, W. B. *Dalton Trans.* **2001**, 2215. (b) Dechy-Cabaret, O.; Martin-Vaca, B.; Bourissou, D. *Chem. Rev.* **2004**, *104*, 6147. (c) Williams, C. K.; Hillmyer, M. A. *Polym. Rev.* **2008**, *48*, 1. (d) Thomas, C. M. *Coord. Chem. Rev.* **2010**, *39*, 165. (e) Stanford, M. J.; Dove, A. P. *Chem. Soc. Rev.* **2010**, *39*, 486. (f) Dijkstra, P. J.; Du, H.; Feijen, J. *Polym. Chem.* **2011**, *2*, 520. (g) Dutta, S.; Hung, W.-C.; Huang, B.-H.; Lin, C.-C. *Adv. Polym. Sci.* **2012**, *245*, 219. For reviews dealing with immortal polymerizations, see: (h) Aida, T.; Inoue, S. *Acc. Chem. Res.* **1996**, *29*, 39. (i) Ajellal, N.; Carpentier, J.-F.; Guillaume, C.; Guillaume, S.; Helou, M.; Poirier, V.; Sarazin, Y.; Trifonov, A. *Dalton Trans.* **2010**, *39*, 8363.

(2) (a) Le Borgne, A.; Vincens, V.; Jouglard, M.; Spassky, N. *Macromol. Chem., Macromol. Symp.* **1993**, *73*, 37. (b) Spassky, N.; Wisniewski, M.; Pluta, C.; Le Borgne, A. *Macromol. Chem. Phys.* **1996**, *197*, 2627. (c) Ovitt, T. M.; Coates, G. W. *J. Am. Chem. Soc.* **2002**, *124*,

1316. (d) Zhong, Z.; Dijkstra, P. J.; Feijen, J. *Angew. Chem., Int. Ed.* **2002**, *41*, 4510. (e) Zhong, Z.; Dijkstra, P. J.; Feijen, J. *J. Am. Chem. Soc.* **2003**, *125*, 11291. (f) Nomura, N.; Ishii, R.; Akahura, M.; Aoi, K. *J. Am. Chem. Soc.* **2002**, *124*, 5938. (g) Nomura, N.; Ishii, R.; Yamamoto, Y.; Kondo, T. *Chem. Eur. J.* **2007**, *13*, 4433. (h) Tang, Z.; Chen, X.; Pang, X.; Yang, Y.; Zhang, X.; Jing, X. *Biomacromolecules* **2004**, *5*, 965.

(3) (a) Pang, X.; Chen, X.; Du, H.; Wang, X.; Jing, X. *J. Organomet. Chem.* **2007**, *692*, 5605. (b) Alaaeddine, A.; Thomas, C. M.; Roisnel, T.; Carpentier, J.-F. *Organometallics* **2010**, *29*, 491. (c) Bouyahi, M.; Grunova, E.; Marquet, N.; Kirillov, E.; Thomas, C. M.; Roisnel, T.; Carpentier, J.-F. *Organometallics* **2008**, *27*, 5815.

(4) (a) Hormniru, P.; Marshall, E. L.; Gibson, V. C.; White, A. J. P.; Williams, D. J. *J. Am. Chem. Soc.* **2004**, *126*, 2688. (b) Hormnirun, P.; Marshall, E. L.; Gibson, V. C.; Pugh, R. I.; White, A. J. P. *Proc. Natl. Acad. Sci. U.S.A.* **2006**, *103*, 15343. (c) Du, H.; Velders, A. H.; Dijkstra, P. J.; Sun, J.; Zhong, Z.; Chen, X.; Feijen, J. *Chem. Eur. J.* **2009**, *15*, 9836.

(5) Whitelaw, E. L.; Loraine, G.; Mahon, M. F.; Jones, M. D. *Dalton Trans.* **2011**, *40*, 11469.

(6) For the ROP of lactide: (a) Iwasa, N.; Fujiki, M.; Nomura, K. *J. Mol. Catal. A: Chem.* **2008**, *292*, 67. (b) Papparlardo, D.; Annunziata, L.; Pellecchia, C. *Macromolecules* **2009**, *42*, 6056. (c) Zhang, W.; Wang, Y.; Sun, W.-H.; Wang, L.; Redshaw, C. *Dalton Trans.* **2012**, *41*, 11587. For the ROP of ε-caprolactone: (d) Nomura, N.; Aoyama, T.; Ishii, R.; Kondo, T. *Macromolecules* **2005**, *38*, 5363. (e) Liu, J.; Iwasa, N.; Nomura, K. *Dalton Trans.* **2008**, 3978. (f) Iwasa, N.; Katao, S.; Liu, J.; Fujiki, M.; Furukawa, Y.; Nomura, K. *Organometallics* **2009**, *28*, 2179.

(7) For the use of aluminum complexes supported by tridendate Schiff base {NOO} ligands, see: (a) Darensbourg, D. J.; Karroonnirun, O. *Organometallics* **2010**, *29*, 5627. (b) Darensbourg, D. J.; Karroonnirun, O.; Wilson, S. J. *Inorg. Chem.* **2011**, *50*, 6775. (c) Matsubara, K.; Terata, C.; Sekine, H.; Yamatani, K.; Harada, T.; Eda, K.; Dan, M.; Koga, Y.; Yasuniwa, M. *J. Polym. Sci. A: Polym. Chem.* **2012**, *50*, 957.

(8) (a) Pietrangelo, A.; Hillmyer, M. A.; Tolman, W. B. *Chem. Commun.* **2009**, 2736. (b) Pietrangelo, A.; Knight, S. C.; Gupta, A. K.; Yao, L. J.; Hillmyer, M. A.; Tolman, W. B. *J. Am. Chem. Soc.* **2010**, *132*, 11649.

(9) (a) Peckermann, I.; Robert, D.; Englert, U.; Spaniol, T. P.; Okuda, J. *Organometallics* **2008**, *27*, 4817. (b) Peckermann, I.; Kapelsky, A.; Spaniol, T. P.; Okuda, J. *Inorg. Chem.* **2009**, *48*, 5526. (c) Buffet, J.-C.; Okuda, J.; Arnold, P. L. *Inorg. Chem.* **2010**, *49*, 419.

(10) Blake, M. P.; Schwarz, A. D.; Mountford, P. *Organometallics* **2011**, *30*, 1202.

(11) (a) Douglas, A. F.; Patrick, B. O.; Mehrkhodavandi, P. *Angew. Chem., Int. Ed.* **2008**, *47*, 2290. (b) Acosta-Ramirez, A.; Douglas, A. F.; Yu, I. S.; Patrick, B. O.; Diaconescu, P. L; Mehrkhodavandi, P. *Inorg. Chem.* **2010**, *49*, 5444. (c) Osten, K. M.; Yu, I.; Duffy, I. R.; Lagaditis, P. O.; Yu, J. C. C.; Wallis, C. J.; Mehrkhodavandi, P. *Dalton Trans.* **2012**, *41*, 8123. (d) Xu, C.; Yu, I.; Mehrkhodavandi, P. *Chem. Commun.* **2012**, *48*, 6806. (e) Broderick, E. M.; Guo, N.; Vogel, C. S.; Xu, C.; Sutter, J.; Miller, J. T.; Meyer, K.; Mehrkhodavandi, P.; Diaconescu, P. L. *J. Am. Chem. Soc.* **2011**, *133*, 9278. (f) Yu, I.; Acosta-Ramirez, A.; Mehrkhodavandi, P. *J. Am. Chem. Soc.* **2012**, *134*, 12734.

(12) Hu, M.; Wang, M.; Zhang, P.; Wang, L.; Zhu, L.; Zhu, F.; Sun, L. *Inorg. Chem. Commun.* **2010**, *13*, 968.

(13) Dagorne, S.; Normand, M.; Kirillov, E.; Carpentier, J.-F. *Coord. Chem. Rev.* **2013**, DOI: j.ccr.2013.02.012.

(14) Normand, M.; Kirillov, E.; Roisnel, T.; Carpentier, J.-F. *Organometallics* **2012**, *31*, 1448.

(15) Effective ionic radii for four-coordinate metal centers: Al^{3+}, 0.39 Å; In^{3+}, 0.62 Å. Shannon, R. D. *Acta Crystallogr., Sect. A* **1976**, *A32*, 751.

(16) (a) Chamberlain, B. M.; Cheng, M.; Moore, D. R.; Ovitt, T. M.; Lobkovsky, E. B.; Coates, G. W. *J. Am. Chem. Soc.* **2001**, *123*, 3229. (b) Bouyahyi, M.; Ajellal, N.; Kirillov, E.; Thomas, C. M.; Carpentier, J.-F. *Chem. Eur. J.* **2011**, *17*, 1872 and references cited therein.

(17) Grunova, E.; Kirillov, E.; Roisnel, T.; Carpentier, J.-F. *Dalton Trans.* **2010**, *39*, 6739.

(18) Avinash, T., N.; Huang, Y.; Viresh, R. H. *Org. Lett.* **2007**, *9*, 3873.

(19) Kirillov, E.; Roisnel, T.; Razavi, A.; Carpentier, J.-F. *Organometallics* **2009**, *28*, 2401.

(20) Runge, F.; Zimmermann, W.; Pfeiffer, H.; Pfeiffer, I. *Z. Anorg. Allg. Chem.* **1952**, *267*, 39.

(21) (a) Kopasz, J. P.; Hallock, R. B.; Beachley, O. T. *Inorg. Synth.* **1986**, *24*, 89. (b) Beachley, O. T.; MacRae, D. J.; Churchill, M. R.; Kovalevsky, A. Y.; Robirds, E. S. *Organometallics* **2003**, *22*, 3991. (c) Peckermann, I.; Robert, D.; Englert, U.; Spaniol, T. P.; Okuda, J. *Organometallics* **2008**, *27*, 4817.

(22) During the attempts to grow single crystals from saturated diethyl ether solutions of $\{ON^{CH2mes}\}AlMe_2$ (**1h**), adventitious traces of water reacted with the dimethylaluminum complex to give the μ,μ-dihydroxy bis(monomethylaluminum) derivative $[(\{ON^{CH2mes}\}AlMe(\mu\text{-}OH)]_2$ (**4h**). Only a few crystals of this compound were recovered. Its solid-state structure, showing a C_2-symmetric compound where both aluminum centers are in a five-coordinated distorted-square-pyramidal geometry (τ = 0.21), bonded to two bridging hydroxyl moieties and coordinated with one phenoxy-imine ligand, is reported in the Supporting Information (Figure S71).

(23) Calculated from the equation $\tau = (\beta - \alpha)/60$. See: Addison, A. W.; Rao, T. N.; Reedjik, J.; Van Rijn, L.; Verschoor, G. C. *J. Chem. Soc., Dalton Trans.* **1984**, 1349. The τ value ranges from 0 (perfectly square pyramidal) to 1 (perfectly trigonal bipyramidal). α and β are the angles that are opposite each other in the *xy* plane (with the In−X bond oriented along the *z* axis).

(24) Acosta-Ramírez, A.; Douglas, A. F.; Yu, I.; Patrick, B. O.; Diaconescu, P. L.; Mehrkhodavandi, P. *Inorg. Chem.* **2010**, *49*, 5444.

(25) Normand, M.; Kirillov, E.; Roisnel, T.; Carpentier, J.-F. *Organometallics* **2012**, *31*, 5511.

(26) For examples of discrete aluminum lactate complexes related to the ROP of lactides, see: (a) Reference 2g. (b) Dagorne, S.; Le Bideau, F.; Welter, R.; Bellemin-Laponnaz, S.; Maisse-Francois, A. *Chem. Eur. J.* **2007**, *13*, 3202. (c) Lewinski, J.; Horeglad, P.; Wojcik, K.; Justyniak, I. *Organometallics* **2005**, *24*, 4588.

(27) It must be noted still that the validity of these comparisons remains limited, since different reaction temperatures and also different batches of solvent/monomer/alcohol were used in these studies and that the TOF data were not necessarily all determined at the same conversion values.

(28) Ding, K.; Miranda, M. O.; Moscato-Goodpaster, B.; Ajellal, N.; Breyfogle, L. E.; Hermes, E. D.; Schaller, C. P.; Roe, S. E.; Cramer, C. J.; Hillmyer, M. A.; Tolman, W. B. *Macromolecules* **2012**, *45*, 5387.

(29) Huang, Y.; Wang, W.; Lin, C. C.; Blake, M. P.; Clark, L.; Schwarz, A. D.; Mountford, P. *Dalton Trans.* **2013**, DOI: 10.1039/C3DT50135C.

(30) All those tacticity values did not change significantly over the polymerization course: that is, for a given system, they were found constant within experimental reproducibility and analytical uncertainty (±0.03) for monomer conversion in the range 30−90%.

(31) Peckermann, I.; Kapelski, A.; Spaniol, T. P.; Okuda, J. *Inorg. Chem.* **2009**, *48*, 5526.

(32) Compounds **3a**−**m**, when used with 10 equiv of alcohol (Table 5, entries 12−17), provided much narrower distributions than compound **2m** under similar conditions (entry 11). Although this was not investigated in more detail, this observation might reflect the different tendencies of the dimethylindium vs bis((trimethylsilyl)methyl)indium compounds (which do not react with alcohol/lactide under these reaction conditions; see text) in promoting transfer and/or transesterification side reactions.

(33) The range of catalyst concentration was limited by the low solubility of complex **3m**.

(34) Avinash, T., N.; Huang, Y.; Viresh, R. H. *Org. Lett.* **2007**, *9*, 3873.

(35) Beachley, O. T., Jr.; Rusinko, R. N. *Inorg. Chem.* **1979**, *18*, 1966.

(36) Bürger, H.; Cichon, J.; Goetze, U.; Wannagat, U.; Wismar, H. J. *J. Organomet. Chem.* **1971**, *33*, 1.
(37) (a) Mehrotra, A.; Mehrotra, R. C. *Inorg. Chem.* **1972**, *11*, 2170. (b) Bradley, D. C.; Chudzynska, H.; Frigo, D. M.; Hammond, M. E.; Hursthouse, M. B.; Mazid, M. A. *Polyhedron* **1990**, *9*, 125. (c) Neumüller, B.; Heravi, M. M.; Chamazi, N. N. *Z. Anorg. Allg. Chem.* **2006**, *636*, 2043.
(38) Kowalski, A.; Duda, A.; Penczek, S. *Macromolecules* **1998**, *31*, 2114.
(39) (a) Altomare, A.; Burla, M. C.; Camalli, M.; Cascarano, G.; Giacovazzo, C.; Guagliardi, A.; Moliterni, A. G. G.; Polidori, G.; Spagna, R. *J. Appl. Crystallogr.* **1999**, *32*, 115. (b) Sheldrick, G. M. *SHELXS-97, Program for the Determination of Crystal Structures*; University of Göttingen, Göttingen, Germany, 1997. (c) Sheldrick, G. M. *SHELXL-97, Program for the Refinement of Crystal Structures*; University of Göttingen, Göttingen, Germany, 1997. (d) Sheldrick, G. M. *Acta Crystallogr.* **2008**, *64*, 112.
(40) Farrugia, L. J. *J. Appl. Crystallogr.* **1999**, *32*, 837.